BASEMENT DELINEATION IN INDO-GANGETIC ALLUVIAL PLAINS BASED ON GRAVITY DATA

A DISSERTATION

Submitted in partial fulfillment of the
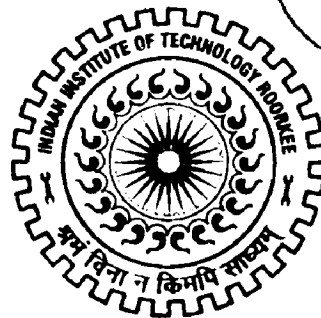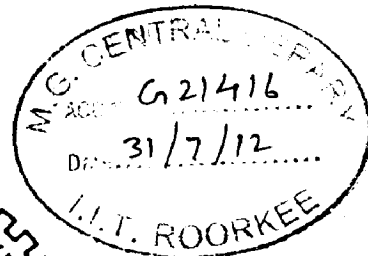*requirements for the award of the degree*
of
MASTER OF TECHNOLOGY
in
GEOPHYSICAL TECHNOLOGY
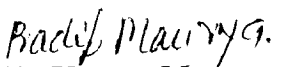
By
PRADIP KUMAR MAURYA

DEPARTMENT OF EARTH SCIENCES
INDIAN INSTITUTE OF TECHNOLOGY ROORKEE
ROORKEE - 247 667 (INDIA)
JUNE, 2012

CANDIDATE'S DECLARATION

I hereby declare that the work which is being presented in this dissertation, entitled 'Basement Delineation in Indo-Gangetic Alluvial Plains Based on Gravity Data' in the partial fulfillment of the requirement for the award Master of Technology in Geophysical Technology submitted in Department of Earth Sciences, Indian Institute of Technology, Roorkee, carried out during a period of July 2011 to April 2012 under the supervision of Dr. Rambhatla G. Sastry, Professor, Department of the Earth Sciences, Indian Institute of Technology, Roorkee.

The matter embodied in this dissertation has not been submitted by me for the award of any other degree.
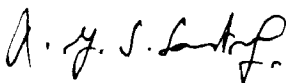
Dated: 15th June 2012
Place: IIT Roorkee

Pradip Maurya

Pradip Kumar Maurya

This is to certify that the above statement made by the candidate is correct to the best of my knowledge.

signature

Dr. Rambhatla G. Sastry
(Supervisor)
Professor of Geophysics
Department of Earth Sciences
Indian Institute of Technology
Roorkee-India

Dated: 14/06/2012
Place: IIT Roorkee

2

Abstract

Till date, basement tectonics delineation through gravity in Indo-Gangetic Plains is limited to constant density contrast models. Here, an attempt is made to use variable density variation with depths for basement delineation in IGP using gravity.

Based on published Bouguer gravity anomaly data, the basement configuration of a part of Indo-Gangetic Plains is deciphered with the help of 3D gravity inversion algorithm. This algorithm accounts for variable density contrast variation with depth, and calculate the depth of density interface using the residual anomaly data. Basement depth map has been derived from the gravity. The basement exhibits a block structure bounded by many faults and having several local highs and lows. The proposed Delhi-Haridwar ridge seems to be simplistic concept and it extends upto Muzaffarnagar. Several depocentres have been observed in the study region. A NW-SE trending fault parallel to HFT has also been demarcated

The study indicates that basement faults run parallel to HFT and orthogonal to it thereby leading to blocky structure with various depocentres. These basement faults can be linked to Himalayan orogeny

Acknowledgement

This dissertation is the result of my last year work whereby I have been helped and supported by many people. It's a matter of great pleasure to acknowledge the help I have had in completing the dissertation work.

It is my delightful duty to express my gratitude to Prof. R.G.S Sastry for his able supervision and expert guidance throughout the present work. His constructive criticism will remain as a prized asset for me.

I am very thankful to Prof. H. Sinvhal to give me opportunity to present my work. And also I would like to express my gratefulness to Prof P. K. Gupta and Prof A. K. Saraf for providing necessary facilities during their respective periods as the Head of the Department

I remained indebted to Mr. Shivendra Kumar Yadav who helped me in different ways

Lastly I would like to thank my entire classmates for their supports during the dissertation works

Pradip kuamr Maurya

4

Contents

Chapter 1- Introduction

Chapter-2 Forward Gravity Modeling

Chapter-4 Study Region

Chapter-5 Gravity Data processing

LIST OF FIGURES

INTRODUCTION

1.1 General

Thanks to natural physical field mapping including gravity, it has enabled us to gather information about interior of the earth.

Gravity anomaly, which we record, is always a composite of contributions from all depths within the usual range of exploration interest (Dobrin and Savit, 1988). Our objective in interpretation is to gain information about the individual contributing sources. This is very difficult task considering the fact that gravity prospecting focus the problem of non-uniqueness. Thus the gravity data demands the great deal of intuition, both physical and geological, and it is useful if the information from the other geophysical sources are available. Without taking into account additional information from available geophysical and geological methods, gravity interpretation may be wrong.

However the gravity method is important not just from exploration point of view, but it became an important tool to study geodynamics problems. The Indo-Gangetic plain is a case in point.

1.2 Review of literature

The Indo-Gangetic plains are regarded as a major unit in Indian sub-continent lying between the peninsular India and extra Peninsular India (Fig 1.1). The origin of the Himalayas and the alluvium covered plains has been studying in the past to present. Edward Suess was first to suggest that the Indo-Gangetic depression is a 'fore deep'
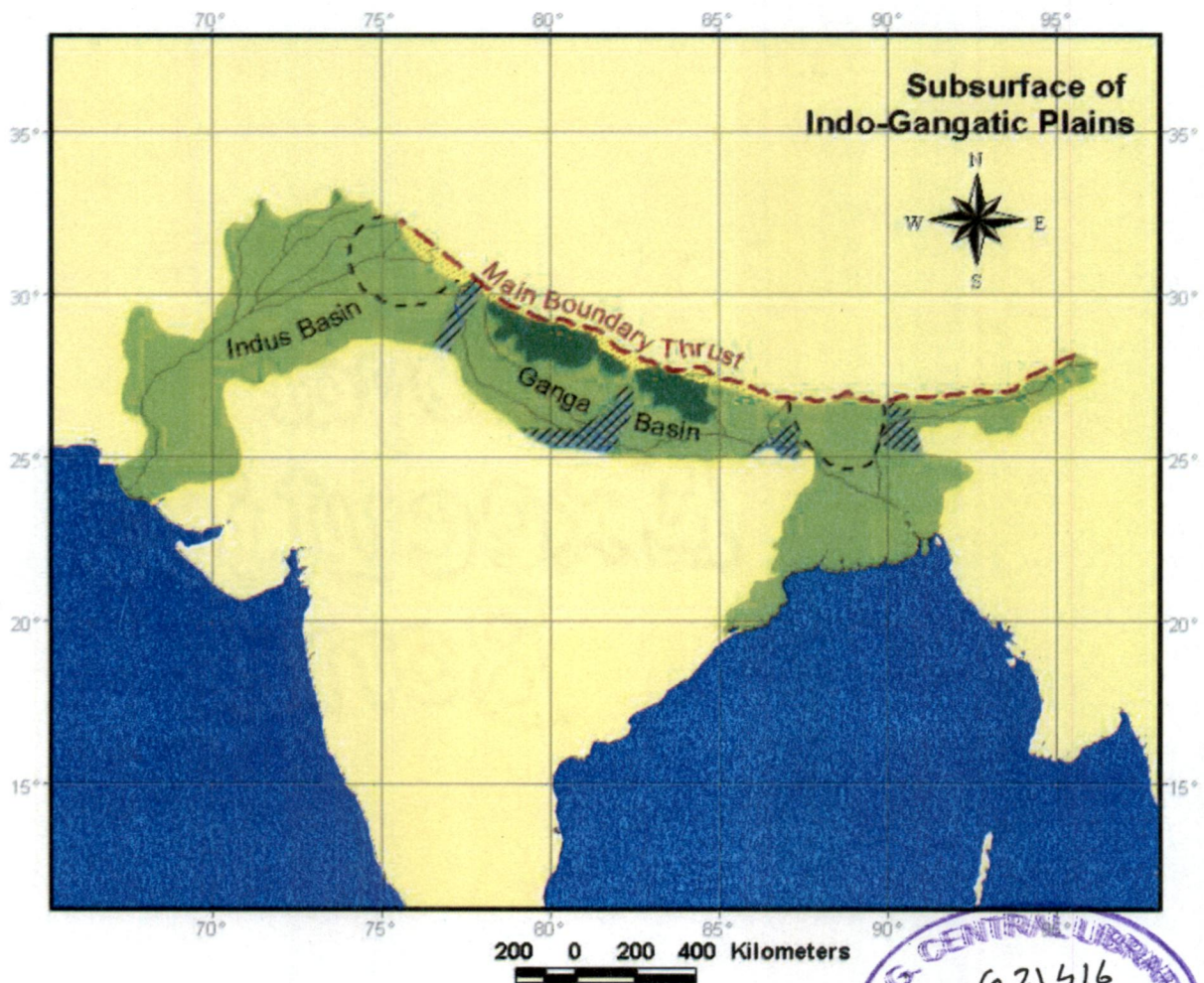
Fig.(1.1) Location Of Indo-Gangetic Plains In Map of India

(source- http://www.iitk.ac.in/gangetic/images/subsurf_lindo-gang%28crop%29.jpg)

formed in front of high crust wave of the Himalaya as they are registered in their southward advance by the rigid landmass of the peninsular (Wadia, 1957). On the basis of the geodetic observation, Bullard (1915) suggested that the Himalayan folds are the results of the under thrusting of the Indian sub-crust below the land mass of the central Asia and the Gangetic area has been represented by a rift or fracture that runs several thousand feet in the earth sub crust which has been filled up by detrital deposits.

10

SCALE

Miles 96 48 16 0   .96 Miles

LEGEND

5000	BASEMENT DEPTH IN FEET
	SIWALIK DHARMSALA (DAGSHAI & KASAULI) GROUPS & SUBATMU FORMATION (TERITARY)
V V V	DECCAN TRAP (CRETACEOUS - EOCENE)
V V V	RAJMAHAL TRAP (JURASSIC)
	GONDWANA (CARSCNIFEROUS - JURASSIC)
	VINDHYANS (LOWER CAMBRIAN)
	DELHI / ARAVALLI (ARCHAEAN - ALGONKIAN)
+ + +	GRANITES / UNCLASSIFIED CRYSTALLICES
▲ ▲	FAULTS
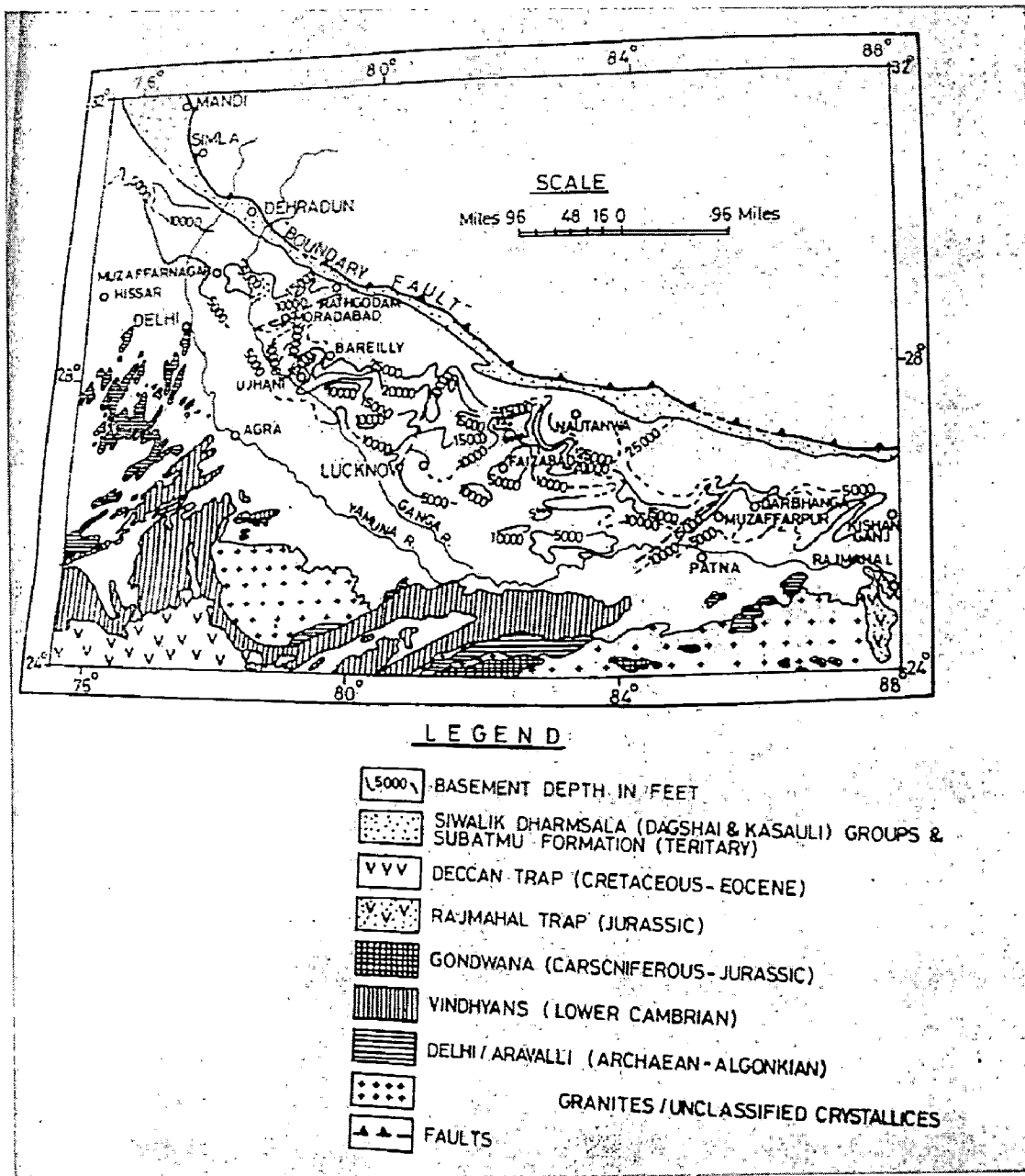
Fig (1.2) Basement structure and depths of Indo-gangetic plains as estimated from airborne magnetometer survey (after Agocs, 1956)

Like the structure and the tectonics of the Indo-Gangetic plains has drawn the attention of geoscientists, the question regarding the basement configuration (Sengupta, 1977 Ramchandra Rao, 1973 Agrawal, 1977, Sastry et al., 1971). Earth scientists have been exploring about the deep structures in the area. ONGC has carried out a lot of

11

geophysical work in this area (sengupta, 1977 ;Agrawal,1977; Rao,1973). Later the Indo-Gangetic plain has gained the importance in geodynamics.

By considering the regional gravity data, Molnar (1988) has suggested that the Indo-Gangetic plain is not in isostatic equilibrium. The negative anomaly over the plains is caused by the low density sediments as well as the flexture of the Indian plate below the plains.

The general basement configuration of the plains gained priority in the minds of the earth scientist when geophysical work first started in the plains. Agocs (1957) interpreted the areo- magnetic survey data in terms of certain local highs and lows of the basement. Sengupta (1977) has attempted to estimate the geological implications of the local highs and lows of the basement. A look at the basement contour map based on the aero-magnetic data shows that the basement is not structurally uniform north- west to south-east and it is segmented by basement knobs or faults or both. The regional trend of the contours, which is north-west to south-east (Fig 1.2). As the major part of the basin follows the trend of Himalayas and is most probably the effect of Himalayan orogeny. Over these regional features are impressed a number of local highs and lows all of which plunge to the north-east these trends seem to follow those of Archeans in peninsular India. Sengupta (1977) associates these north-east plunging ones to post–Delhi movement. The basement depth contour map Fig (1.2) shows the plains has segmented into four basins which are follows:

(I) A basin of shallow to medium depth beginning from north west of Moradabad and extending upto the border of west Pakistan or beyond

(II)   A deep basin starting from near Moradabad and extending through Bareily, Sahajanpur, Hardoi and Lucknow upto longitude 82° east. The basin is separated from the first one by a fault just east of Moradabad.

(III) A deep basin stretching from NE of Faizabad to Motihari and separated from the basin described above by a basement high known as Faizabad ridge.

12

(IV) A basin of intermediate depth (upto 1500 feet) east of Darbhanga and Extending upto 88°E longitude. This basin is separated from the above basin by a NE-SW fault passing north or north east of the Patna and the basement high east of Darbhanga.
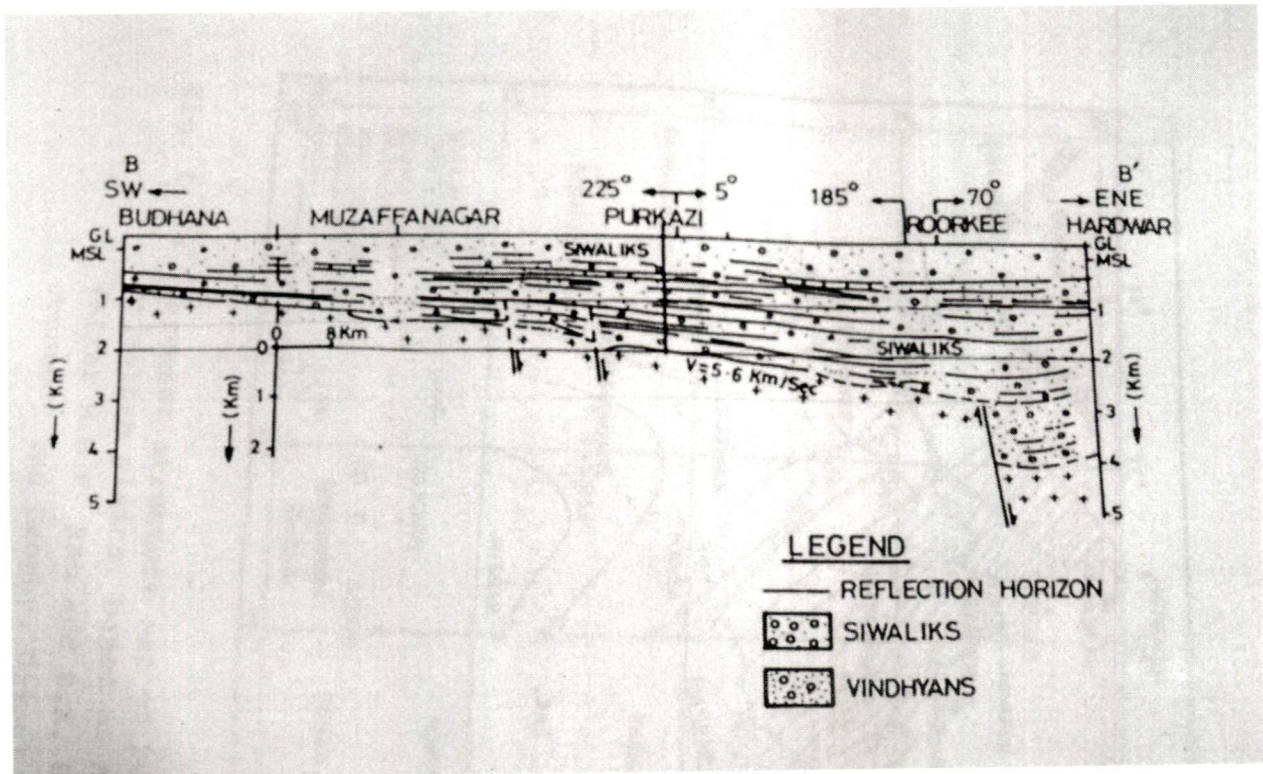
Fig 1.3 Seismic section along Muzaffarnagar-Roorkee (Agrawal, 1977)

Agrawal (1977) has summarized the results on the basis of Gravity, Magnetic and seismic data. On the basis of oldest sediments overlying the basement, the Indo-Gangetic plains can be divided into three basins, where Siwaliks, Vindhyans and Gondwanas respectively overlie the basements. In the southern part of the Ganga and Purnea basin (where well data is available), the Siwaliks overlie the Vindhyans and Gondwana with a major unconformity. In the Punjab plains the seismic survey does not show the presence of any major fault affecting either the basement or the overlying sediments. The nature and attitude of the basement remains same throughout Punjab plains and to the east upto Muzaffarnagar- Roorkee The seismic section along Muzaffarnagar –Roorkee shows some minor basement faults.(Fig 1.3). Refraction surveys near Saharanpur have recorded a

13

refractor with a boundary velocity of 5.6 km/sec. This refractor seems to corresponds to the basement. The seismic section shows that the thickness of sedimentary column increases 1.1 from Budhana in the SE to nearly 3.4 km in the north. The increase in sedimentary column is corroborated by fig (1.4)
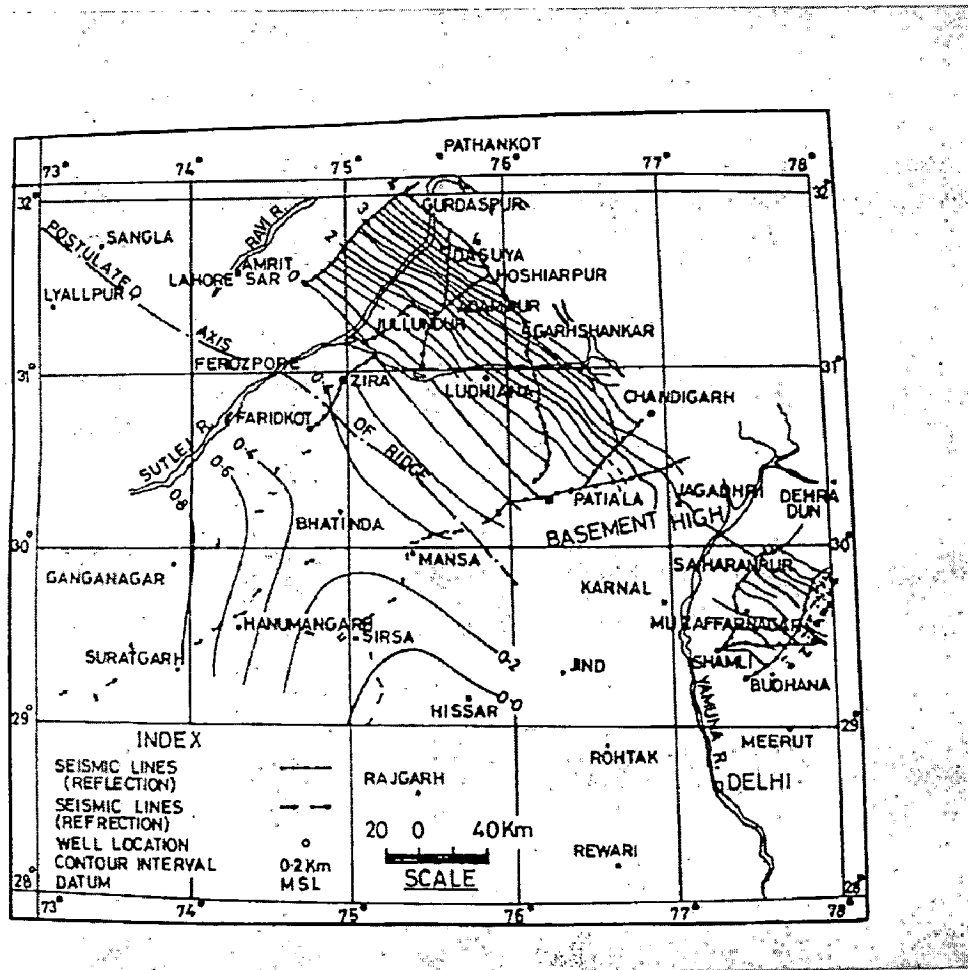
Fig (1.4) Basement structure map of Punjab- Rajasthan Plains based on seismic data (after Rao and Gupta 1964, courtesy Indian geophysics union)

The seismic data of Ganga basin suggests that the possibility of its division into two independent basins designated as the west Uttar Pradesh (including Uttarakhand) and East Uttar Pradesh basin by a subsurface ridge termed as Faizabad ridge. The Monghyr-Saharsa ridge separates the Ganga basin and Purnea basin. As regards the western margin of the Ganga basin and the Purnea basin, there are a lot of debates. According to

14

Agrawal, (Gupta, 1971) while interpreting the residual anomaly suggest the extension of Aravalli under the alluvium divides the Ganga and Punjab basins. This is disputed by Agrawal (1977) and Ramchandra Rao (1973), who suggest that the basement high known as Kalka-Ambala uplift divides the Punjab and Ganga basins.

Regional geophysical studies in Ganga Plains fore land basin shows a number of highs and ridges as well as faults (Sastri et al., 1973; Rao,1971;Agrawal,1977). From south important basement highs are Delhi-Haridwar-Ridge, Faizabad Ridge, a poorly developed Mirzapur- Ghazipur ridge, Monghyr-Saharsa Ridge, while the Raxual, Bahriach and Puranpur regions exist as basement highs in northern part of basin These basement highs represent more rigid part and have resisted the down-flexing of the foreland basin. Therefore sediment thickness is much reduced over these ridges than in adjacent areas. For example, thicknes of alluvium near Lucknow is about 2.0 km. At Rai-Barielly the basement is found at 474 m in one borehole in the Faizabad ridge.

The important basement faults are; Muradabad fault, Bareilly fault the Lucknow fault, the Patna fault and the Malda fault. There is no surface expressions of these faults or any control on geomorphic features and seem to be inactive basement faults (Agrawal 1977)

A number of workers have delineated the basement structures in western part of Uttar Pradesh and Uttarakhand (Sastry,et al.,1971; Rao,1973;Agrawal 1977). In this context the Delhi- Haridwar ridge(DHR) has been described as buried extension of the Aravallis (tectonic map of india ONGC,1968) which according to others extends deep into the Himalaya and affect the tectonics during the India-Asia collision (Valdia,1973,1978; Raiverman et al., 1983) However the bouguer anomaly map of the region shows a nose like structure . Based on this observation, Rao (1973) has questioned the extension of the DHR beyond Shamili. Further the deep well drilled at Mohand (15km south of Dehradun) did not touch the crystalline basement even at a depth of 5.26 km. The work of Rao

(1973), Sengupta (1977) and Agrawal (1977) suggests that the basement dips gently northwards

Mishra and Luxman (1997) have carried out spectral analyses of the Bouguer gravity anomaly of western part of Ganga basin and concluded that the basement exhibits block structure with several basement ridges such as Delhi –Haridwar, Delhi-Moradabad and Agra –Saharanpur, Which are genetically related to basement blocks uplifts. Further they suggested east-west tectonics of the Ganga- Basin might be caused by collision of Indian and Eurasian palate (Mishra and Laxman, 1977). This collision has caused the development of foreland basin in front of the rising Himalayan belt, where pre- Tertiary Lesser Himalayan sequences override the evolving basin along the Main Boundary Thrust (MBT). In turn, the dominant Siwalik Group sequences within the basin override the Indo-Gangetic Plains along the Himalayan Frontal Thrust (HFT) as results of the Himalayans tectonics.

The geophysical investigation in Indo-Gangetic alluvium plains was carried out by Sastry et.al., (1999). Based on the gravity and magnetic observation they suggested that the basement exhibits a block structure bounded by many faults, several highs and lows in the study regions. According to them widely-held Delhi- Haridwar ridge is too simplistic model for the basement structure. The maximum northern limit of extension up to Muzaffarnagar towards south. Further they concluded that the HFT related tectonics has affected the basement much before the surface expression of the HFT at the geomorphic interface between the IGP and the Sub-Himalayan foothills. With the help of two sets of parallel regional gravity and magnetic profiles they had shown the presence of two major additional faults in the HFT region. Lithological composition of the Pre-Tertairy basement around HFT could be inferred based on the correlation between the pair of magnetic anomalies (Fig 1.5)

However, earlier workers have not considered the depth-wise variation of density as density contrasts is constant in their analysis

16
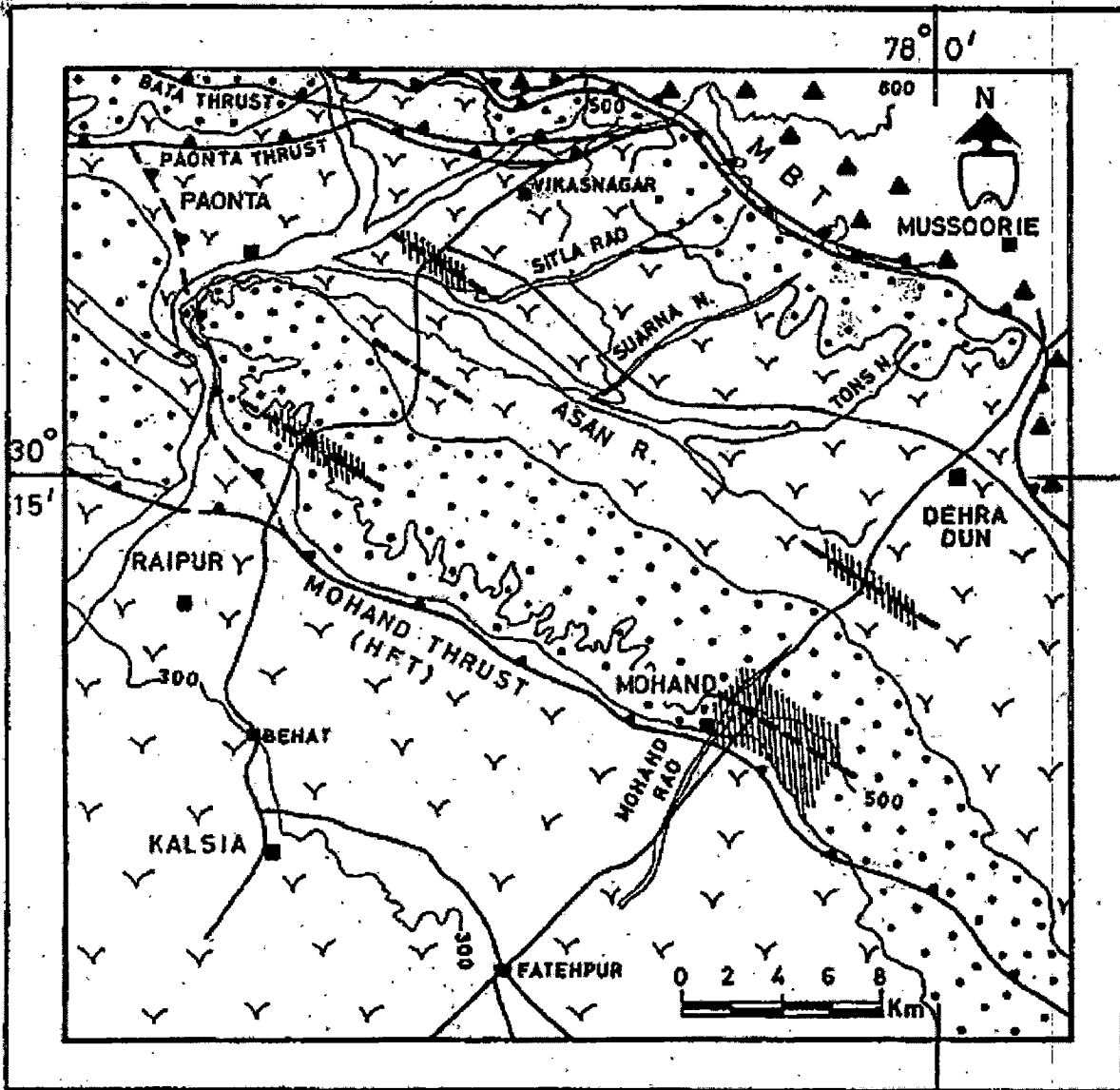
Fig 1.5 Inferred location of fault zones from two sets of regional gravity and magnetic profiles on the geological map (Sastry et al., 1999)

17

1.3 Objectives of the present work

In view of the above, the main objective of present thesis is aimed at delineation of basement configuration of Indo-Gangetic Plains from published Gravity data.

This involves the generation of 3D Gravity inversion algorithm, where density contrast is varying continuously with depth and input residual gravity data with possible regional – residual separation.

1.4 Plan of the Thesis work

Chapter-1 deals with introduction

Chapter-2 discuss the forward modeling for 2D, 2.5D and 3D body using variable density contrast

Chapter-3 deals with the 3D gravity inversion algorithm

Chapter-4 gives a brief account for geology and related tectonics of the Indo-Gangetic plains

Chapter-5 discusses the processing of gravity data

Chapter-6 outlines of derived results and discussion

Chapter-7 provides the summary and conclusions

CHAPTER 2

FORWARD GRAVITY MODELING

2.1 General

Forward modeling of a geophysical geometry involve the computation of the theoretical geophysical response of the model. Problems of Gravity interpretation of a sedimentary basin could be overcome by assigning a mathematical geometry to the anomaly causing body with a known density contrast. Most of the available algorithms that employ mathematical geometries, assume that the density of sedimentary rocks above the basement interface is uniform, and therefore, a constant density contrast is generally taken in the modeling schemes (Morgan and Grant, 1963; Bhattacharya and Navolio, 1975). However, field studies show that the density of sedimentary rocks increases progressively with depth therefore, it creates different density contrast at different depth i.e. density contrast varying with depth. So inclusion of density function that depends on depth can improve the results in comparison with constant density approach. As already discussed in the introduction part various density function were proposed in literature by several authors. In which parabolic density function is suited best in recent years.

Here is outlined forward gravity modeling of 2D, 2.5D and 3D body with variable density function. Parabolic density function given by Chakravarthi and Rao (1993), one can have,

$$\Delta\rho(z) = \frac{\Delta\rho_0^3}{(\Delta\rho_0 - \alpha z)^2},$$

(2.1)

where $\Delta\rho(z)$ is the density contrast of a section of a sedimentary column at any depth z, $\Delta\rho_0$ is the density contrast observed at the ground surface i.e., at z= 0 and α is a constant, which needs to be find out from the known density data of the study region.

2.2 2D Forward Gravity modeling

The analytical gravity expression for two-dimensional arbitrary shaped body (shown in Fig 2.1) with PDC (parabolic density contrast) can be given as (Visweswara Rao et al., 1994)

$$\Delta g(0) = \sum_{k=1}^{N} dg(k)$$

(2.2)

Where $\Delta g(0)$ is the gravity value at any point p(0) on principle profile section and dg(k) is the gravity contribution of the kth side of the polygon given by

$$dg(k) = 2G_u \Delta \rho_0^3 \left\{ \frac{\phi'_{k+1}}{\alpha s2} - \frac{\phi'_k}{\alpha s1} + \frac{B(T2 - T1)}{2A\alpha} \right.$$
$$\left. - \frac{C \sin i}{A} \ln \left(\frac{S2 r_k}{S1 r_{k+1}} \right) \right\}.$$

(2.3)

Here

$$S1 = \Delta \rho_0 - \alpha z_k,$$

$$S2 = \Delta \rho_0 - \alpha z_{k+1},$$

$$R = ((x_{k+1} - x_k)^2 - (z_{k+1} - z_k)^2)^{1/2},$$

$$\sin i = (z_{k+1} - z_k)/R,$$

$$\cos i = (x_{k+1} - x_k)/R,$$

$$C = x_k \sin i - z_k \cos i,$$

$$A = C^2 \alpha^2 + 2\Delta \rho_0 \alpha C \cos i + \Delta \rho_0^2,$$

$$B = -2C\alpha \cos i - 2\Delta\rho_0,$$

$$T1 = \arctan((z_k + C \cos i)/C \sin i),$$

$$T2 = \arctan((z_{k+1} + C \cos i)/C \sin i)$$

and

$$r_k = (x_k^2 + z_k^2)^{1/2},$$

$$r_{k+1} = (x_{k+1}^2 + z_{k+1}^2)^{1/2},$$

$$\phi_k' = \Pi/2 - \phi_k,$$

$$\phi_{k+1}' = \Pi/2 - \phi_{k+1}$$

G_u is the universal gravitational constant Here ϕ_{k+1} and ϕ_k the angles made at the point of calculation by the radial vector r_k and r_{k+1}, of the vertices of the kth side of the polygon with the principal profile.
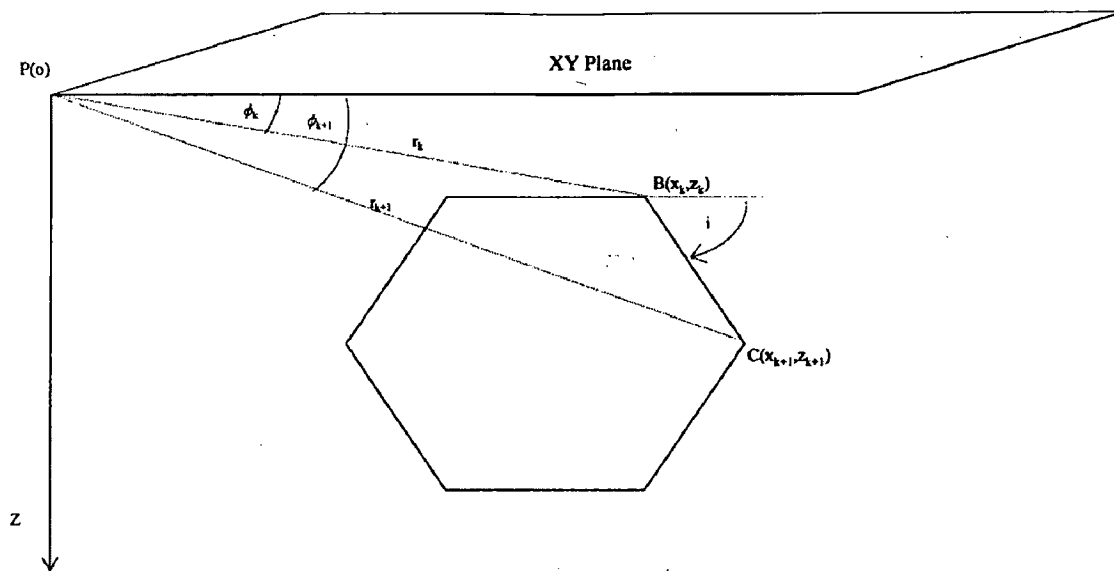
Fig. 1. Two-dimensional polygonal cross-section.

Fig 2.1 Two-dimensional polygon cross-section (Chakravarthi et al., 2001)

It can be noted that if we want to calculate gravity based on constant density then we have to put $\alpha = 0$ in eq.(1)so that $\Delta\rho(z)$ becomes $\Delta\rho(0)$ and Using eq. (2.2) and (2.3) we can calculate gravity response of a two-dimensional polygon with uniform density. To avoid the singularity eq. (2.3) can be written as

$$dg(k) = \frac{2G_u\Delta\rho_0^3}{A}\left\{\frac{\phi'_{k+1}(z_{K+1}F1 + CF2)}{s2} - \frac{\phi'_k(z_kF1 + CF2)}{s1} + C\sin i\ln\left(\frac{S1r_{k+1}}{S2r_k}\right)\right\}$$

where

$$F1 = \Delta\rho_0 + \alpha C\cos i,$$

$$F2 = \Delta\rho_0 \cos i + \alpha C$$

(2.4)

In general, the gravity contribution $dg_m(k)$ of the kth side of the polygon at any point x_m on the principal profile can be calculated by substituting $x_k - x_m$ and $x_{k+1} - x_m$ respectively, in eq (4), eq.(2.2) becomes as

$$\Delta g(x_m) = \sum_{k=1}^{N} dg_m(k).$$

(2.5)

And now by assigning the coordinates and using the eq.(2.4) and eq.(2.5) gravity anomaly of a sedimentary basin can be calculated. This is how the forward modeling is done using the variable density contrast.

2.3 2.5D Forward modeling

The geometry of 2.5D vertical prism is shown in Fig 2.2 considering this Figure let vertical axis (z-axis) be perpendicular to the plane of the paper and positive inward with

d_1 and d_2 as depths to top and bottom of the prism, respectively. Let the x-axis be the transverse to the strike of the prism Let 2S and 2b be the strike length along the y-axis and width along the x-axis, respectively Further, let the profile, RR *, be transverse to the strike of the model and bisect it. Let us assume R (0,0) to be the origin which is placed vertically above the Centre of the prism, then the gravity anomaly at any point, P (x_k, 0), on the profile can be expressed as

$$g\left(x_k, 0\right) = \int_{w=d_1}^{d_2} \int_{v=-S}^{S} \int_{u=-b}^{b} \frac{G\,\Delta\rho(w)\,w\,du\,dv\,dw}{\left[(u - x_k)^2 + v^2 + w^2\right]^{3/2}}$$

(2.6)

where G is universal gravity constant and $\Delta\rho(w)$ is the density contrast given by a parabolic density function at a given depth same as eq. (2.1). Now using equation (2.1) and (2.6) we can obtain expression of gravity anomaly which can be given as

$$g(x_k, 0) = -2G\Delta\rho_0^3 \Bigg[\Bigg\{ \frac{\alpha x_k S}{t_4}\left(\frac{1}{t_2} + \frac{1}{t_3}\right)\ln\frac{t_5}{t_6} + \frac{S}{2t_2}\ln\frac{(R + x_k)}{(R - x_k)} + \frac{x_k}{2t_3}\ln\frac{(R + S)}{(R - S)}$$
$$+ \frac{\Delta\rho_0}{\alpha}\left\langle \frac{1}{t_2}\tan^{-1}\frac{SR}{w\,x_k} + \frac{1}{t_3}\tan^{-1}\frac{x_k R}{wS}\right\rangle - \frac{1}{\alpha t_5}\tan^{-1}\frac{Sx_k}{wR}\Bigg\}_{x_k-b}^{x_k+b} \Bigg]_{d_1}^{d_2}.$$

(2.7)

$R = \left(x_k^2 + S^2 + w^2\right),$
$t_1 = x_k^2 + S^2,$
$t_2 = S^2\alpha^2 + \Delta\rho_0^2,$
$t_3 = x_k^2\alpha^2 + \Delta\rho_0^2,$
$t_4 = \sqrt{t_1\alpha^2 + \Delta\rho_0^2},$
$t_5 = \Delta\rho_0 - \alpha w,$

and

$t_6 = -2(\alpha R\,t_4 + t_1\alpha^2 + \Delta\rho_0\,\alpha w).$
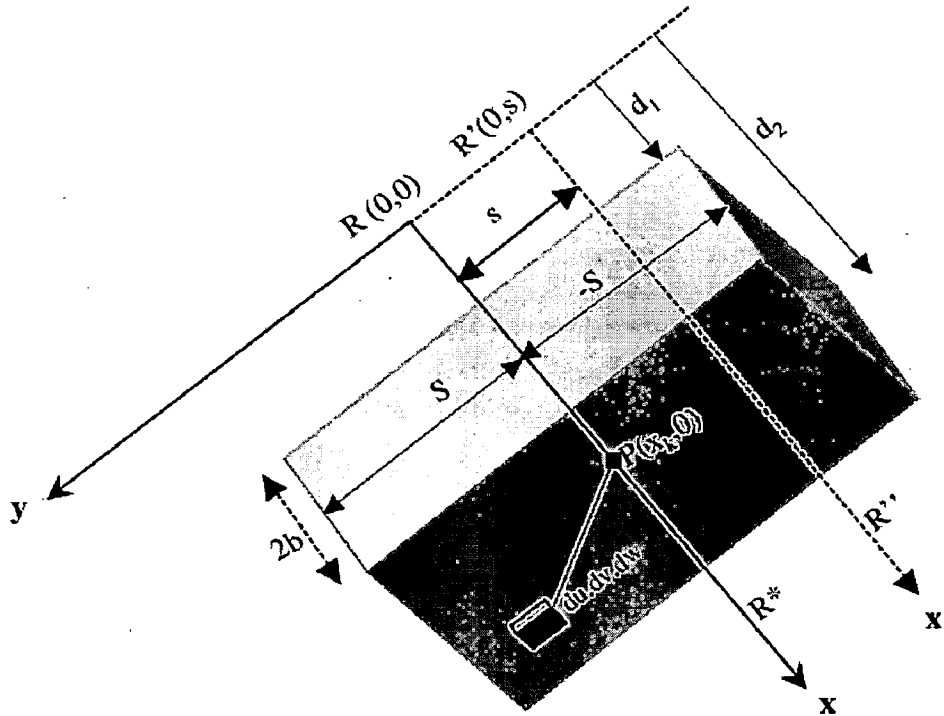
Fig 2.2 Geometry of a 2.5D vertical prism (Chakravarthi et al.,2002)

Using eq. (2.7) we can compute the gravity anomaly along the profile RR when it is running through origin. Gravity anomaly at any point having offset distance s, from the origin can be obtained by replacing S by S-s and S+s and then averaging it. We can use the eq.(2.7) to compute gravity anomaly when density contrast is constant . In this case we need to put $\alpha=0$ in density function. In such a case eq. (2.7) will reduce to

$$
g(x_k, 0) = 2\,G\Delta\rho_0 \left[\left\{ z \tan^{-1} \frac{Y x_k}{zR} + \frac{Y}{2} \ln \frac{(R + x_k)}{(R - x_k)} - \frac{x_k}{2} \ln \frac{(R + Y)}{(R - Y)} \right\}_{x_k-b}^{x_k+b} \right]_{d_1}^{d_2} \cdot
$$

(2.8)

2.4 3D Forward modeling

In this context we assume the sedimentary load is approximated by juxtaposed right rectangular prism. The geometry is shown in the Fig (2.3). The analytical expression of the sedimentary basin at any grid node (i, j) is of a rectangular mesh is given as (Chakravarthi et al. 2002)

$$g_{sbasin}(i,j,0) = \sum_{k=2}^{NOY-1} \sum_{l=2}^{NOX-1} g_{PRISM}k, l,$$

(2.9)

Where NOX and NOY are the no. of grid nodes along X and Y axis respectively, and g_{PRISM} is the gravity anomaly due to single prism, which can be derived using parabolic density function as described below,
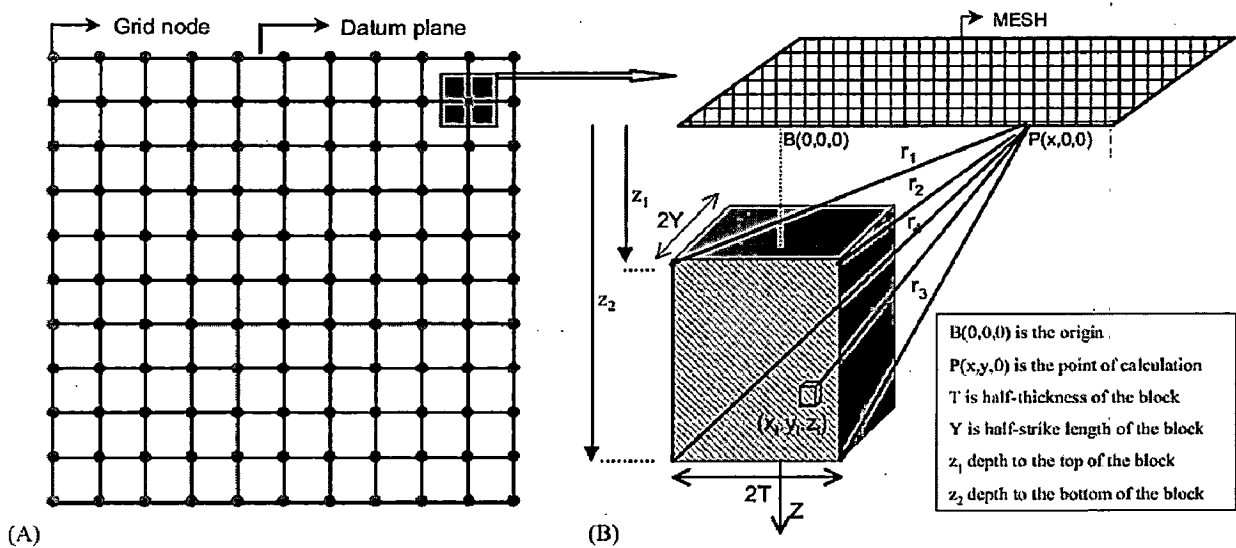
(Chakravarthi et. al.,2002)

Fig. 2.3(A) Geometry of a rectangular/square mesh with top view of a 3-D building block (B) Geometry of 3-D building block

Let us suppose, 2T (width of the prism), 2Y (strike length of the prism), Z_1 (depth to the top of the prism), Z_2 (depth to the bottom of the prism) are the dimensions of a 3-D vertical prism as shown in Fig. 2.3. Let the density contrast along the prism decreases

vertically according to Eq. (2.1) Now Placing the origin B(0,0,0) vertically above the centre of the prism, the gravity anomaly at a point P(x,0,0) on the XY plane can be obtained by integrating the gravity effect of a 3-D element volume x_1 y_1 z_1 throughout the volume of the prism and can be expressed as

$$g_{PRISM}(x, 0, 0)$$

$$= G\,\Delta\rho(z) \int_{z_1}^{z_2} \int_{-T}^{T} \int_{-Y}^{Y} \frac{z_l\,dx_l\,dy_l\,dz_l}{[(x - x_l)^2 + y_l^2 + z_l^2]^{3/2}}.$$

..........................(2.10)

Substituting Eq. (1) in (2.10) we can get ,

$$g_{PRISM}(x, 0, 0) = G\,\Delta\rho_0^3 \int_{z_1}^{z_2} \int_{-T}^{T} \int_{-Y}^{Y} \frac{1}{(\Delta\rho_0 - \alpha z_l)^2}$$

$$\times \frac{z_l\,dx_l\,dy_l\,dz_l}{[(x - x_l)^2 + y_l^2 + z_l^2]^{3/2}}$$

$$= 2G\,\Delta\rho_0^3 Y \int_{z_1}^{z_2} \int_{x-T}^{x+T} \frac{1}{(\Delta\rho_0 - \alpha z_l)^2}$$

$$\times \frac{z_l\,dx_l\,dz_l}{[x_l^2 + Y^2 + z_l^2]^{1/2}(x_l^2 + z_l^2)}.$$

Now integrating with respect to x between limits x-T and x+T, we have

$$g_{PRISM}(x, 0, 0) = 2G\,\Delta\rho_0^3 \int_{z_1}^{z_2} \frac{1}{(\Delta\rho_0 - \alpha z_l)^2}$$

$$\times \left[\tan^{-1} \frac{Y(x + T)}{z_l\sqrt{(x + T)^2 + Y^2 + z_l^2}} \right.$$

$$\left. -\tan^{-1} \frac{Y(x - T)}{z_l\sqrt{(x - T)^2 + Y^2 + z_l^2}} \right] dz.$$

After full integration we obtain

$$g_{PRISM}(x,\ 0,\ 0)$$

$$= 2G\,\Delta\rho_0^3 \left\{ \frac{\alpha Y(x+T)(2\Delta\rho_0^2 + \alpha^2|Y^2 + (x+T)^2|)}{L_1(Y^2\alpha^2 + \Delta\rho_0^2)(\Delta\rho_0^2 + \alpha^2|x+T|^2)} \right.$$

$$\times \ln \frac{L_3(\alpha r_4 L_1 + L_1^2 - \Delta\rho_0 L_4)}{L_4(\alpha r_1 L_1 + L_1^2 - \Delta\rho_0 L_3)}$$

$$- \frac{\alpha Y(x-T)(2\Delta\rho_0^2 + \alpha^2|Y^2 + (x-T)^2|)}{L_2(Y^2\alpha^2 + \Delta\rho_0^2)(\Delta\rho_0^2 + \alpha^2|x-T|^2)}$$

$$\ln \frac{L_3(\alpha r_3 L_2 + L_2^2 - \Delta\rho_0 L_4)}{L_4(\alpha r_2 L_2 + L_2^2 - \Delta\rho_0 L_3)} - \frac{\Delta\rho_0}{\alpha(\Delta\rho_0^2 + Y^2\alpha^2)}$$

$$\left[\tan^{-1}\frac{Yr_4}{z_2|x+T|} - \tan^{-1}\frac{Yr_1}{z_1|x+T|} \right] + \frac{\Delta\rho_0}{\alpha(\Delta\rho_0^2 + Y^2\alpha^2)}$$

$$\left[\tan^{-1}\frac{Yr_3}{z_2|x-T|} - \tan^{-1}\frac{Yr_2}{z_1|x-T|} \right] - \frac{\Delta\rho_0}{\alpha(\Delta\rho_0^2 + |x+T|^2\alpha^2)}$$

$$\left[\tan^{-1}\frac{|x+T|r_4}{z_2 Y} - \tan^{-1}\frac{|x+T|r_1}{z_1 Y} \right] - \frac{\Delta\rho_0}{\alpha(\Delta\rho_0^2 + |x-T|^2\alpha^2)}$$

$$\left[\tan^{-1}\frac{|x-T|r_3}{z_2 Y} - \tan^{-1}\frac{|x-T|r_2}{z_1 Y} \right] + \frac{Y}{2(\Delta\rho_0^2 + Y^2\alpha^2)}$$

$$\ln\left[\frac{(|x+T|-r_4)(|x+T|+r_1)}{(|x+T|+r_4)(|x+T|-r_1)} \right] + \frac{Y}{2(\Delta\rho_0^2 + Y^2\alpha^2)}$$

$$\ln\left[\frac{(|x-T|-r_3)(|x-T|+r_2)}{(|x-T|+r_3)(|x-T|-r_2)} \right] + \frac{x-T}{2(\Delta\rho_0^2 + |x-T|^2\alpha^2)}$$

$$\ln\left[\frac{(Y-r_3)(Y+r_2)}{(Y+r_3)(Y-r_2)} \right] + \frac{x+T}{2(\Delta\rho_0^2 + |x+T|^2\alpha^2)}$$

$$\ln\left[\frac{(Y-r_4)(Y+r_1)}{(Y+r_4)(Y-r_1)} \right]$$

$$+ \frac{1}{\alpha}\left[\frac{1}{\Delta\rho_0 - \alpha z_2}\left\langle \tan^{-1}\frac{Y|x+T|}{z_2 r_4} - \tan^{-1}\frac{Y|x-T|}{z_2 r_3} \right\rangle \right]$$

$$-\frac{1}{\alpha}\left[\frac{1}{\Delta\rho_0 - \alpha z_1}\left\langle \tan^{-1}\frac{Y|x+T|}{z_1 r_1} - \tan^{-1}\frac{Y|x-T|}{z_1 r_2}\right\rangle\right]\right\}.$$

$$\dots\dots\dots\dots\dots\dots\dots\dots\dots\dots\dots\dots\dots\dots\dots\dots\dots\dots(2.11)$$

Here the expression for the terms used in this main expressions are given below

$$L_1 = \{[(x+T)^2 + Y^2]\alpha^2 + \Delta\rho_0^2\}^{1/2},$$

$$L_2 = \{[(x-T)^2 + Y^2]\alpha^2 + \Delta\rho_0^2\}^{1/2},$$

$$L_3 = \Delta\rho_0 - \alpha z_1,$$

$$L_4 = \Delta\rho_0 - \alpha z_2,$$

and

$$r_1 = [(x+T)^2 + Y^2 + z_1^2]^{1/2},$$

$$r_2 = [(x-T)^2 + Y^2 + z_1^2]^{1/2},$$

$$r_3 = [(x-T)^2 + Y^2 + z_2^2]^{1/2},$$

$$r_4 = [(x+T)^2 + Y^2 + z_2^2]^{1/2},$$

G is universal gravitational constant

Eq. (2.11) is used to compute the theoretical gravity response of one prism and Eq. (2.10) is used to compute total gravity response of the sedimentary basin at point of calculation. Eq. (2.10) is valid for the profile passing through origin . The gravity anomaly at any point offset by a distance y from the origin of the Cartesian co-ordinate system is obtained by averaging the gravity contributions of the prism calculated by putting Y-y and Y+y for Y In Eq. (2.11) .

CHAPTER 3

3D GRAVITY INVERSION ALGORITHM

3.1 General

In gravity prospecting, the study related to regional and hydrocarbon exploration involves the depth calculation of density interfaces from residual gravity fields that are generally attributed to basement relief. Thus, calculating basement depths where the density contrast varies significantly with depth is a problem. Negative gravity anomalies are generally observed over sedimentary basins having a large thickness of low density rocks. It is well known, however, that the interpretation of gravity anomalies is non unique in the sense that the gravity anomalies on the plane of observation can be explained by a variety of density distributions. One way to tackle the ambiguity is to assign an approximate mathematical geometry to the anomalous mass with a known density and then to invert the gravity anomalies for the parameters of the model (Chakravarthi and Sundararajan, 2004). Many continental sedimentary basins have limited strike lengths and finite widths; therefore, approximations of such sedimentary basins by 3D geometries are often justified in the quantitative interpretation of gravity anomalies. Talwani and Ewing (1960), Götze and Lahmeyer (1988), Holstein and Ketteridge (1996), and Singh and Gupta sarma (2001) derive expressions for gravity anomalies attributable to 3D polyhedral bodies using constant density. However, the practical utility of these expressions in analyzing gravity anomalies from sedimentary basins is very limited because (1) the density of sedimentary rocks varies with depth (Li, 2001), Nagihara and Hall(2001), Adriasyah and McMechan(2002), Hinze(2003), García-Ab-deslem (2005) and (2) the depth to the floor of a sedimentary basin is not known a prior information. In general, the density of sedimentary rocks in-creases more rapidly at shallower depths than at deeper depths; hence, variable density functions in modeling and inversion often improve results.

Inversion of gravity anomalies due to a sedimentary basin involves a mathematical calculation in which we try to fit the calculated gravity anomalies with the observed one by adjusting the parameters of the model in an iterative manner using the principle of least square. The present algorithm is based on Marquardt algorithm which estimates the depth of density interface in the sedimentary basin. The forward modeling that is used by the present algorithm has been already described in chapter 3 (section 3.3).

Marquardt Inversion algorithm

The present algorithm has been illustrated by Chakravarthi and Sundararajan (2006), the process of inversion begins by calculating initial depths of the density interface at all inner grid nodes of a rectangular mesh as shown in the following picture
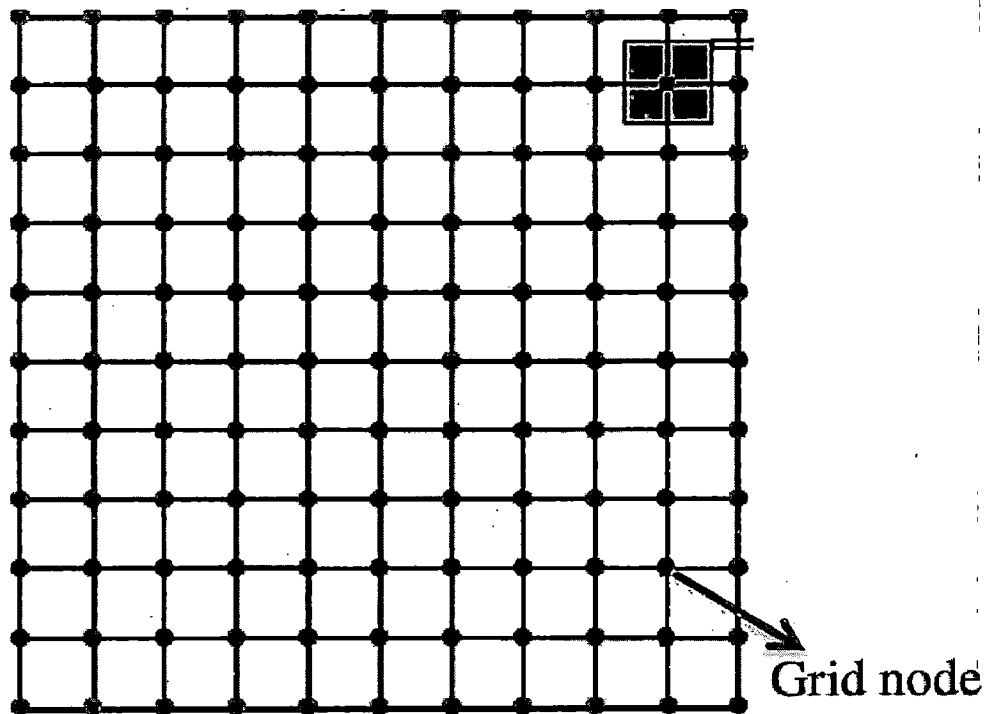

Fig 3.1 Square mesh grid

It is assumed that the observed gravity anomaly It is assumed that the observed gravity anomaly at each grid node (m , n) is being generated by a horizontal infinite slab below the node in which the density contrast varies parabolically with depth (Chakravarthi et

30

al., 2002). The initial depth to the density interface is then calculated based on the expression given by Chakravarthi et al. (2002) as

$$z(m,n) = \frac{g_{obs}(m,n) \cdot \Delta\rho_0}{41.89\Delta\rho_0^2 + \alpha g_{obs}(m,n)},$$

(3.1)

Where m = 2,3,.......NX-1 and n = 2,3 ......NY-1. Here NX and NY are the no. of grid node along X-axis and Y-axis respectively , g_{obs} is our recorded gravity anomaly.

Now the The theoretical gravity anomaly of the density interface $g_{mod}(m, n)$ at any point (x_m, y_n) of a grid node(m ,n) is then calculated using the initial depths given by the Eq. 4.1 as

$$g_{mod(m,n)} = \sum_{k=2}^{NY-1} \sum_{\ell=2}^{NX-1} g_{Prism}(\ell,k).$$

(3.2)

Where g_{PRISM} is the gravity response of a single prism. In general, the modeled gravity anomaly $g_{mod}(m ,n)$ in equation 3.2 deviates from the observed anomaly g_{obs} (m , n) because equation 3.1 calculate only approximate depths. The amount of difference between modeled and observed gravity anomalies at any grid node can be expressed in the following manner

$$[g_{obs(m,n)} - g_{mod(m,n)}] = \sum_{n=2}^{NY-1} \sum_{m=2}^{NX-1} \frac{\partial g_{Prism}}{\partial z} dz_{(m,n)}$$

(3.3)

Here $dz_{(m,n)}$ is the improvement in the depth estimates (our model parameter)

31

An equation similar to equation 3.3 is constructed for each observation, and (NX − 2)(NY − 2) normal equations are framed and solved for the increments to(NX − 2)(NY − 2) prisms by minimizing the quantum of misfit function J , defined by

$$J = \sum_{n=1}^{NY} \sum_{m=1}^{NX} \left[g_{obs(m,n)} - g_{mod(m,n)} \right]^2$$

Now applying the Marquardt's algorithm the system of normal eq. is given by

$$\sum_{n=1}^{NY} \sum_{m=1}^{NX} \sum_{k=1}^{\hat{N}} \frac{\partial g_{(m,n)}}{\partial \hat{P}_{j'}} \frac{\partial g_{(m,n)}}{\partial \hat{P}_k} (1 + \lambda \delta) d\hat{P}_k$$

$$= \sum_{n=1}^{NY} \sum_{m=1}^{NX} \left[g_{obs(m,n)} - g_{mod(m,n)} \right] \frac{\partial g_{(m,n)}}{\partial \hat{P}_{j'}},$$

$$j' = 1,2,\ldots, \hat{N},$$

(3.4)

Where $\check{N}$ is the no. of parameters to be solved and $d\check{P}_k$ are improvements to the depth estimates . λ is the damping factor δ is given by the following manner

$$\delta = \begin{cases} 1 & \text{for } j' = \hat{k} \\ 0 & \text{for } j' \neq \hat{k} \end{cases}.$$

The partial derivative required in the above Eq. (3.4) are given by the following analytical expressions that is derived by differentiating the formula of gravity anomaly of a prism and can be written as

$$\frac{\partial g}{\partial z} = 2G\Delta\rho_0^3 \left\{ \frac{Y\alpha 2}{T3} \left[\frac{(x+T)(2\Delta\rho_0^2 + \alpha^2 T_1)}{L_1 T_6} \right. \right.$$

$$\times \left(\frac{T_4 r_4 + L4(L_1 z + \Delta\rho_0 r_4)}{L_4 r_4 T_4} \right)$$

$$- \frac{(x-T)(2\Delta\rho_0^2 + \alpha^2 T_2)}{L_2 T_7}$$

$$\left. \times \left(\frac{T_5 r_3 + L_4(L_2 z + \Delta\rho_0 r_3)}{L_4 r_3 T_5} \right) \right]$$

$$+ \frac{\Delta\rho_0 Y}{\alpha T_3} \left[\frac{T_1(x+T)}{r_4(z^2(x+T)^2 + Y^2 r_4^2)} \right.$$

$$\left. - \frac{T_2(x-T)}{r_3(z^2(x-T)^2 + Y^2 r_3^2)} \right]$$

$$+ \frac{\Delta\rho_0 Y}{\alpha} \left[\frac{T_1(x+T)}{T_6 r_4(z^2 Y^2 + (x+T)^2 r_4^2)} \right.$$

$$\left. - \frac{T_2(x-T)}{T_7 r_3(z^2 Y^2 + (x-T)^2 r_3^2)} \right]$$

$$- \frac{Yz}{T_3} \left[\frac{(x+T)}{r_4((x+T)^2 - r_4^2)} - \frac{(x-T)}{r_4((x-T)^2 - r_3^2)} \right]$$

$$- Yz \left[\frac{(x-T)}{r_3 T_7(Y^2 - r_3^2)} - \frac{(x+T)}{r_4 T_6(Y^2 - r_4^2)} \right]$$

$$+ \frac{1}{\alpha(\Delta\rho_0 - \alpha z)} \left[Y\left(\frac{(x-T)(z^2 + r_3^2)}{r_3(z^2 r_3^2 + Y^2(x-T)^2)} \right. \right.$$

$$\left. - \frac{(x+T)(z^2 + r_4^2)}{r_4(z^2 r_4^2 + Y^2(x+T)^2)} \right)$$

$$\left. \left. + \frac{\alpha}{(\Delta\rho_0 - \alpha z)} \left(\tan^{-1} \frac{Y(x+T)}{zr_4} - \tan^{-1} \frac{Y(x-T)}{zr_3} \right) \right] \right\}$$

$$(3.5)$$

This approach involves the calculation of the rate of change of the gravity anomaly with respect to each parameter which is to solved. Initially the value of λ is set to an arbitrary value and then eq. (3.4) is solved for increment or decrement of the parameters. Subsequently increment or decrements in the parameters are added to get new parameters and new misfit function is calculated. If the new misfit function is greater than the previous one the value of damping factor is set to doubled and if it is less than it is decreased by $\lambda/2$ .New misfit function will replace previous one . In this way process will repeat to desired iterations . The algorithm automatically terminates in case i) the specified number of iterations completed or ii) the misfit function falls below a predefined allowable error or iii) the damping factor assumes an unusually large value.

CHAPTER 4

STUDY REGION

4.1 General

Our study region comprises the part of Indo-Gangetic plains in western up and Uttarakhand state. Major places that comprises the study region are Muzaffarnagar, Saharanpur, Haridwar area. Published Bouguer gravity map(After rao, 1973) of this area has been taken for the study. In Fig 4.1, the study region is shown with marked rectangle ABCD on a geological map .

4.2 Geology of the area

The Indo-Gangetic alluvial plains are located to the south of Sub-Himalaya and extends upto the Aravalli in the west, Satpura and Vindhyan ranges in the south. This basin was considered to be a foredeep by Suess.

The origin of Indo-Gangetic plains has been a subject of interest since the early 1900s when Burrard(1915) published a paper on the origin of the Indo-gangetic trough or Himalaya foredeep. The Indo-Gangetic Plain is divided into two drainage basins by the Delhi Ridge; the western part consists of the Punjab Plain and the Haryana Plain, and the eastern part consists of the Ganges–Bramaputra drainage systems. This divide is only 300 metres above sea level, causing the perception that the Indo-Gangetic Plain appears to be continuous between the two drainage basins.

The crystalline rocks underlying the basin represents the extension of structural elements of the Indian peninsular shield. Over a large part of the Ganga basin the continental Neogene to Quaternary sediments belonging to the Siwalik formation rest directly over a regional unconformity over the underlying, gently folded Vindhyan sequence. However,

35
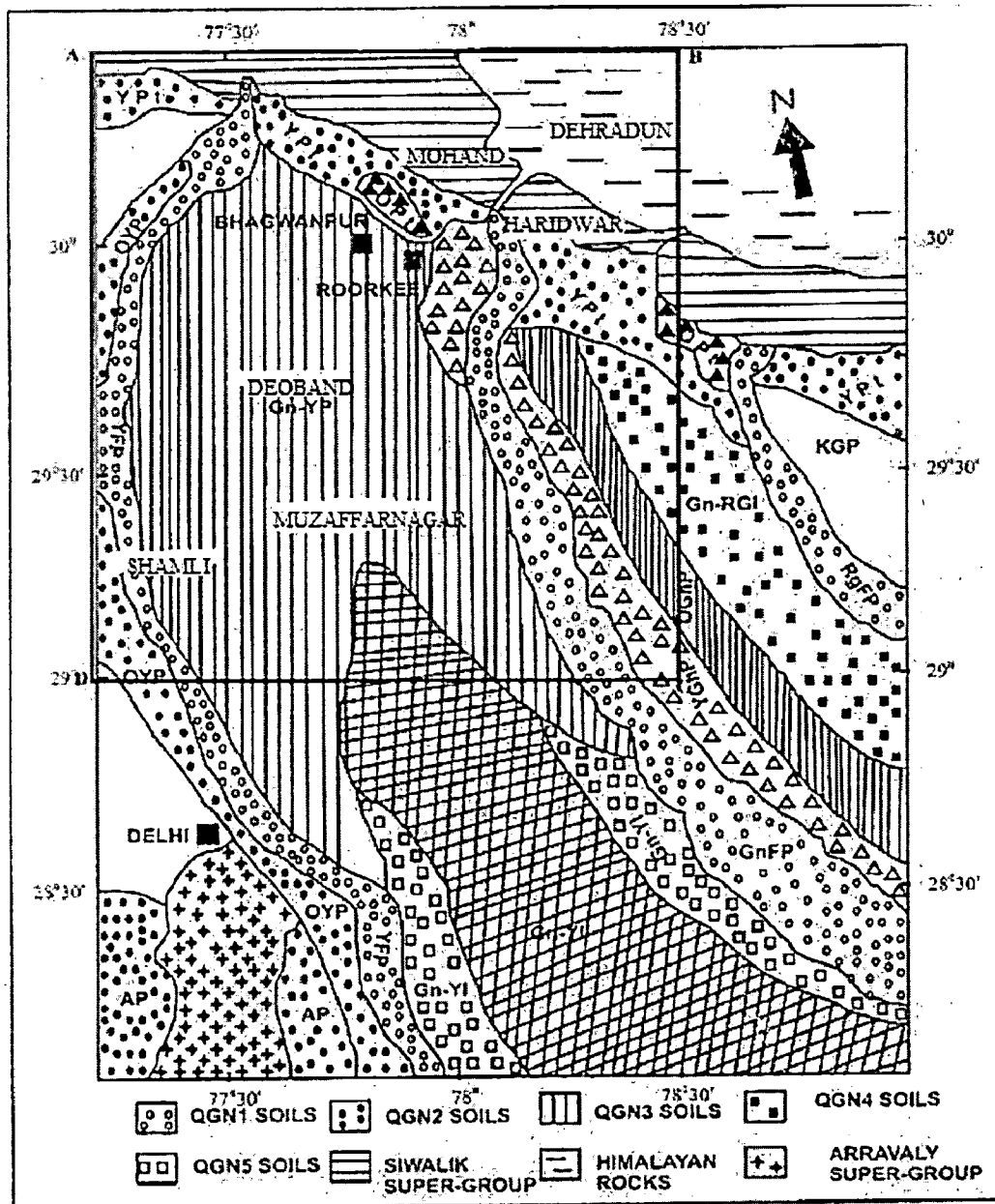
Fig 4.1Study region, shown with marked rectangle ABCD on geological map (Prakash et al., 2000,2001)

GnFp-Ganga Flood Plain; YGP- Young Ganga Plain; OGnP- Old Ganga Plain; GnRGI-Ganga-Ramganga Interfluev; KGP- Koshi-Gola Plain; Gn-YP- Ganga-Yamuna-Plain; GnYI- Ganga-Yamuna-Interfluev, SA- Salt-Affected; NSA- Not Salt-Affected; YPt-Young Piedmont; Opt- Old-Piedmont

underneath the Punjab plains the Siwalik rest directly over the crystalline basement (Agrawal, 1977 : Sastry,1976)

The entire area is covered with a thick blanket of alluvium. The Siwalik Group of rocks range in age from middle Miocene to E. Pleistocene. The rocks are predominantly of continental origin, characterized by a series of orange- coloured clays, coarse grain sandstone and conglomerates, which has been subdivided into the the Lower, middle and upper Siwaliks. ·

4.3 Tectonics of the Indo-Gangetic plains

The Himalayan mountain chain is a product of continent- continent collision between Indian and Asian plates in which Indian plate is under thrusting the Asian plate. One of the landscape formed in this context is the Indo-Gangetic Plain the foreland basin system which is an actively subsiding peripheral foreland basin system.

Indo-Gangetic plain foreland basin (Fig 4.1) is already in mature stage, where the orogenward part of the basin has been uplifted and moved as thrust sheets to produce the Siwalik hills, making a few km to many tens of km wide belt abutting against fluvial plain. Thus Siwalik sediment represents deposits of earlier stages of Himalayan foreland basin which has been deformed .The present-day Indo-Gangetic plain is an area of active sedimentation subjected to compressional stress.
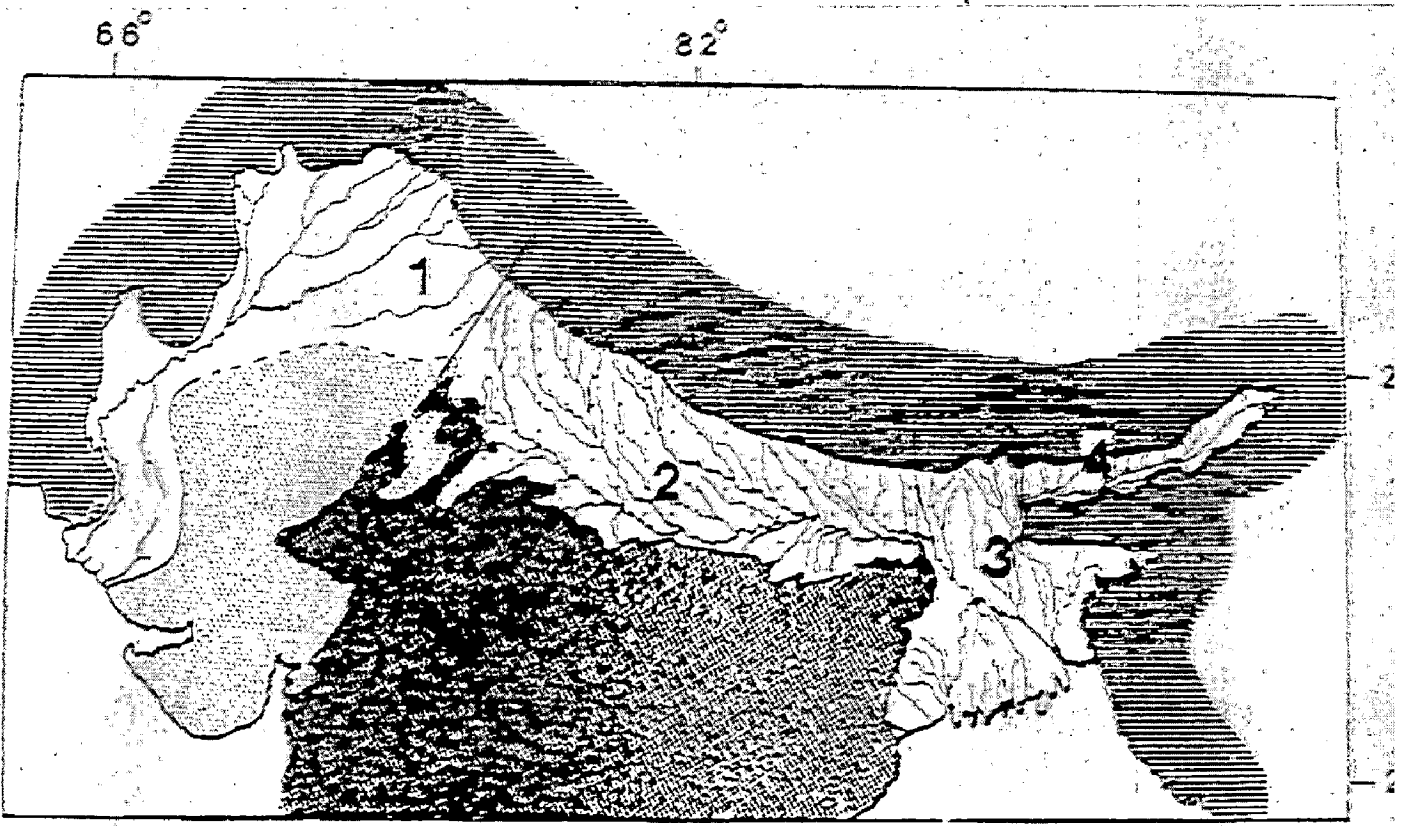
Fig 4.2 Indo-gangetic basin system 1- Punjab- Rajasthan plains 2-Ganga plains 3-Bengal plains 4- Bramhaputra plains (Singh ,1999)

4.4 Basement controls in the Indo-Gangetic plains

The Indian crust beneath the Indo-Gangetic Plains are very old, cold rigid and have many inhomogeneity in the form of basement highs and lows At the same time foreland basin is located at a considerable distance from the Indus suture. Hence despite large scale thrust fold loading in the Himalayas the down flexing of the crust in the Ganga plain is insufficient. The basin fill show only a moderate thickness. As the sediment input in the basement is high, the basin always remained overfilled above see level. Regional geophysical studies shows a number of highs and ridges as well as faults (Sastri et al., 1973) From south ,important basement highs are Delhi-Haridwar-Ridge, Faizabad Ridge, a poorly developed Mirzapur-Ghazipur ridge, Monghyr-Saharsa Ridge, while the Raxual, Bahriach and Puranpur regions exist as basement highs in northern part of basin (Fig 2.3) These basement highs represent more rigid part and have resisted the down-flexing of the

38

foreland basin The important basement faults are; Muradabad faults, Bareilly faults the Lucknow faults, the Patna faults and the malda faults.
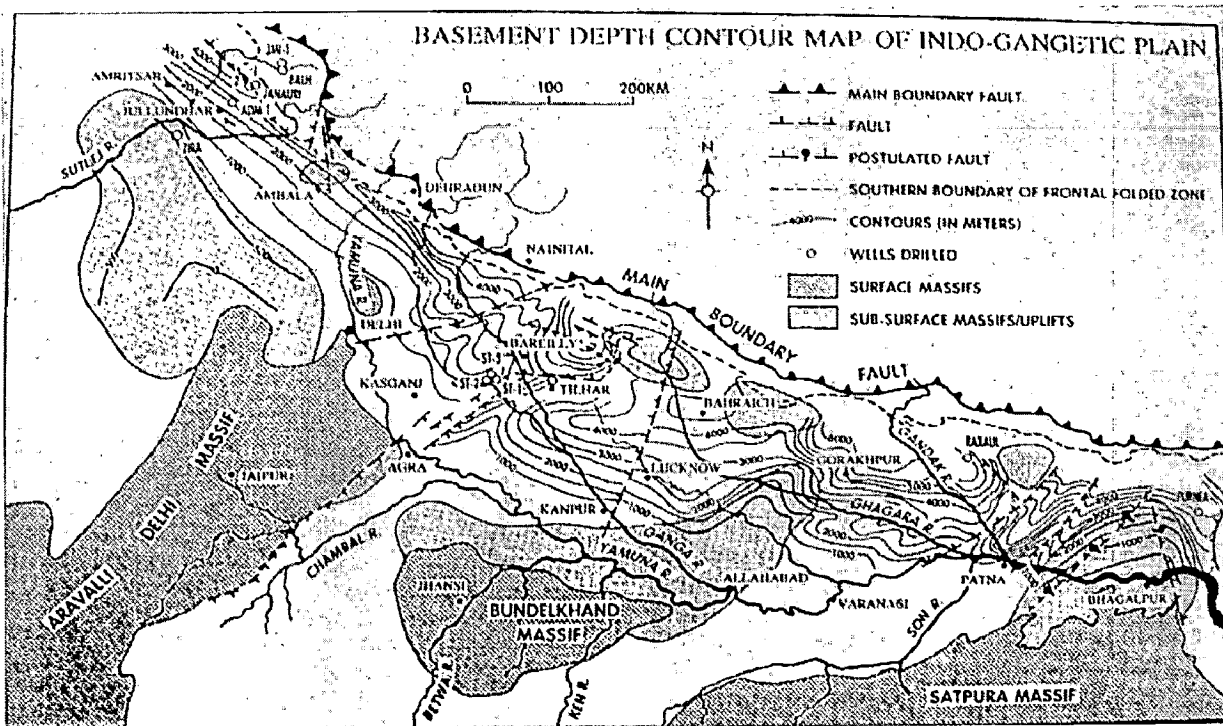

Fig 4.3 Basement map of Ganga Plain showing major basement highs, and depth contours (Simplified after Karunakaran and Ranga Rao)

CHAPTER 5

GRAVITY DATA ANALYSIS

5.1 Gravity data source

For the present work gravity data is taken from a published Bouguer anomaly map of Muzaffarnagar, Saharanpur, Haridwar Area, western U.P (After Rao, 1973). The bouguer anomaly map is shown in Fig (5.1). Here the contour interval is 2mgals and the map scale is 1cm = 10 km.

5.2 Gravity data processing

Since the gravity anomaly value is needed at every grid nodes i.e the gravity value at centre of assumed prism, gravity map is discretize to get the gravity anomaly at each grid nodes taking the grid spacing interval = 1km. The process of digitizing was done manually. The contour map of the digitized data was obtained using the Matlab program and is shown in the Fig (5.2). Further data was extrapolated in required area using Matlab program using spline interpolation model. In Fig.5.2 the extrapolated area has been marked by boundary line around Mohand to Dehradun region and in Barout to south of Sardhana region

Since our algorithm takes the residual value separated from the regional value as input data, we need to further process the data as regional –residual separation from the observed gravity anomaly.
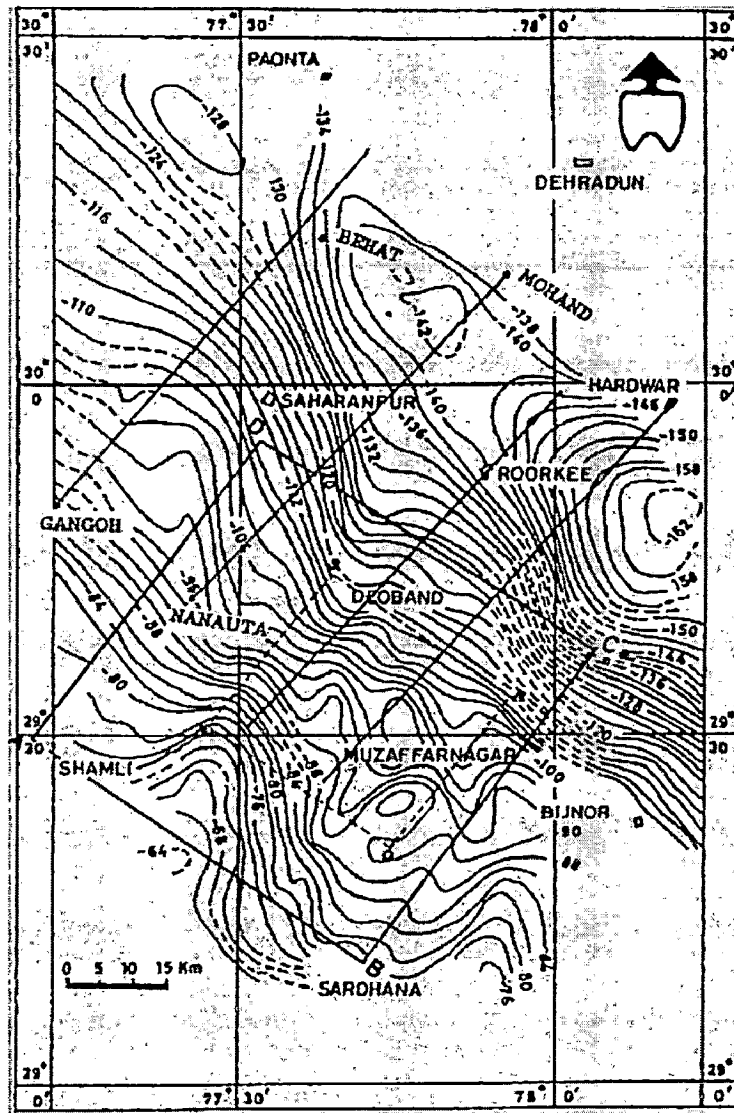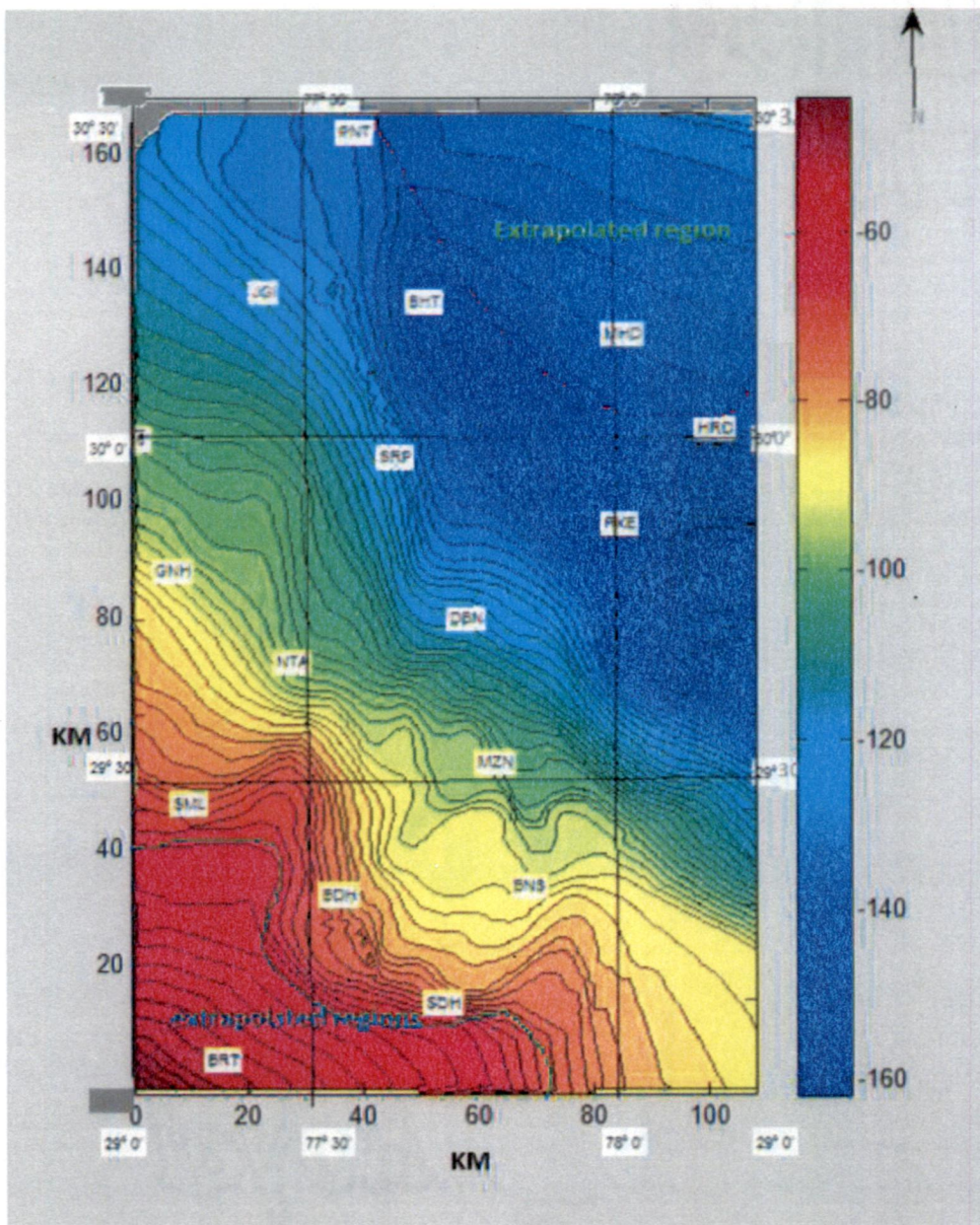
Fig 5.1 Bouguer anomaly map of Muzaffarnagar, Saharanpur, Haridwar Area, western U.P & Uttarakhand (After Rao, 1973)

Fig 5.2 Bouguer anomaly map after discretizing the published map with extra-polated regions marked

Overview of Regional – Residual Separation method

The gravity field is produced generally by the superposition of overlapping gravitational effects of many sources, whose individual anomalies may be difficult to isolate. The terms "residual" and "regional" commonly are used to differentiate between anomalies from local, near surface masses and those arising from larger and generally deeper features, respectively. In many cases, the choice of regional depends on the residual anomalies targeted for interpretation. There are many methods to separate the regional field from the gravity field. According to Nettleton (1976), regional-residual techniques in the analysis of potential field data may be grouped into graphical, spectral, and polynomial fitting method.

The graphical method is slow and cannot be automated. The only constraint imposed on the regional field, besides the interpreter's intuition, is the smoothness. As a result, there will be several solutions to the separation problem, and the inherent subjectivity may be either an advantage or a drawback depending on the interpreter's experience and ability to incorporate relevant geologic information about the regional

Spectral methods on the other hand, provide more quantitative means to characterize the smoothness of a regional field, namely, by its predominantly low-frequency spectral content. They are faster and less subjective than the graphical method because the separation is performed by filtering the total field with a suitable low-pass filter. In applying spectral methods, regional fields may be assumed to be produced either by wide or deep-seated sources. However, due to the overlap of the regional and residual spectra, a complete separation is not possible and two kinds of errors, signal distortion and noise transmission, are always present. Signal distortion is the elimination of part of the signal spectral content by a filtering operation. Noise transmission is the incomplete removal of the noise by a filtering procedure. The total sum of these two errors can be minimized by using a Wiener filter, as shown by Jacobsen (1987). However, any spectral method which

assigns null spectral content to the zero frequency in the residual (and this is the rule) will produce residuals contaminated by pseudo anomalies (Ulrych, 1968). These pseudo anomalies have the opposite sign from the real residual anomaly. They arise because assigning a null spectral content to the residual zero frequency is equivalent to obtaining a residual with a null spatial mean. In other words, there must always be residual anomalies of both signs even though the real residual anomaly may be of just one sign.

Polynomial fitting methods assume that a polynomial surface adequately models the regional field whose smoothness is controlled by the polynomial order (Agocs, 1951; Simpson, 1954), Here the observed data are used to compute, usually by least squares, mathematically describe the surface giving the closest fit to the gravity anomaly that can be obtained within a specified degree of details. This surface is considered to be regional gravity field and is separated from the observed one to get residual anomaly

In the present work the regional –residual separation has been done using

I) Fitting the regional field as a first order polynomial, i.e, considering the regional field is being produced by planner surface (Fig 5.3)

II) Fitting the regional field as a second order polynomial, i.e., considering the regional fields being produced by second order curved surface (Fig 5.4)

A computer program has been designed to compute the residual value using above two methods and is included in Annexture-I.
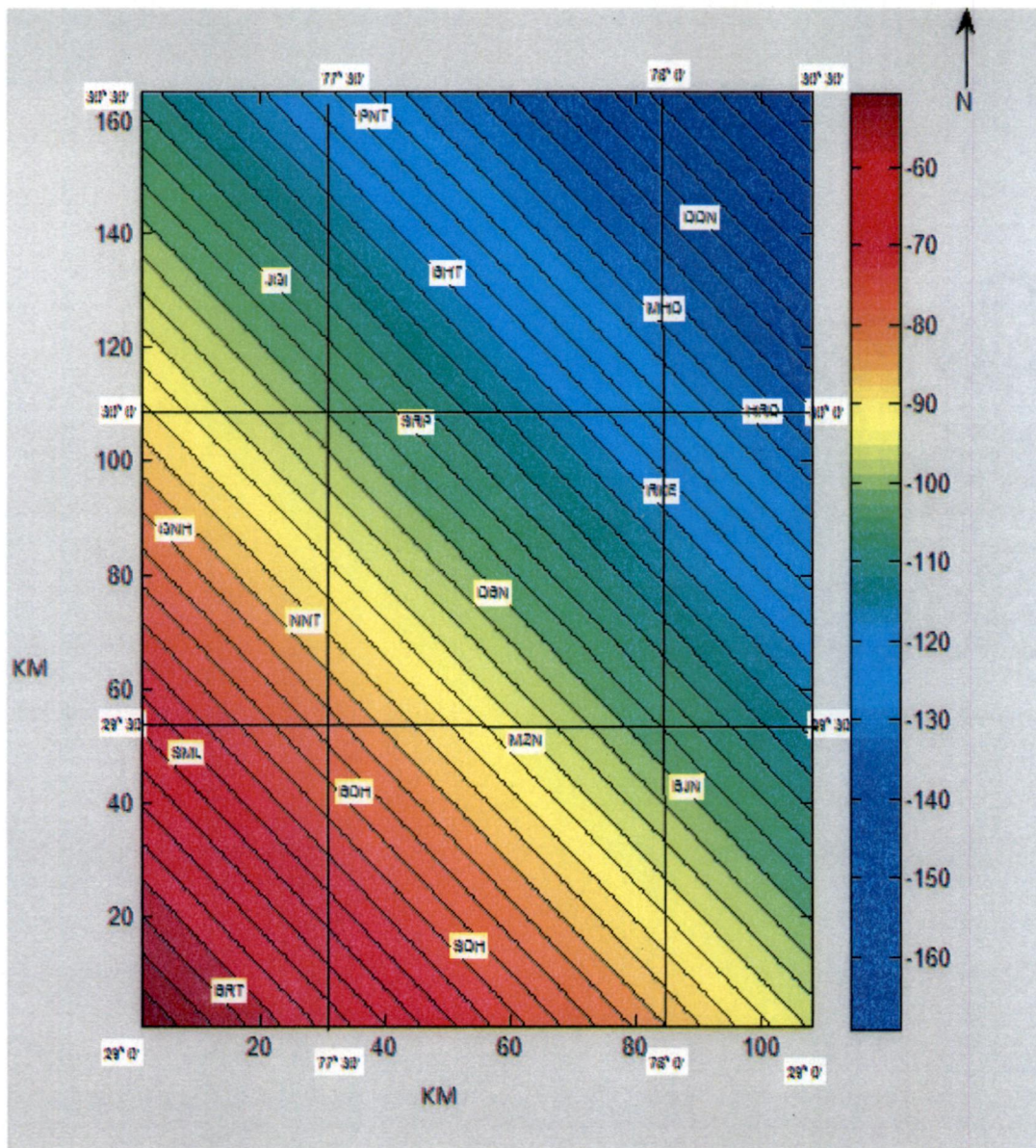
Fig 5.3   Regional gravity map (derived using First order Polynomial)
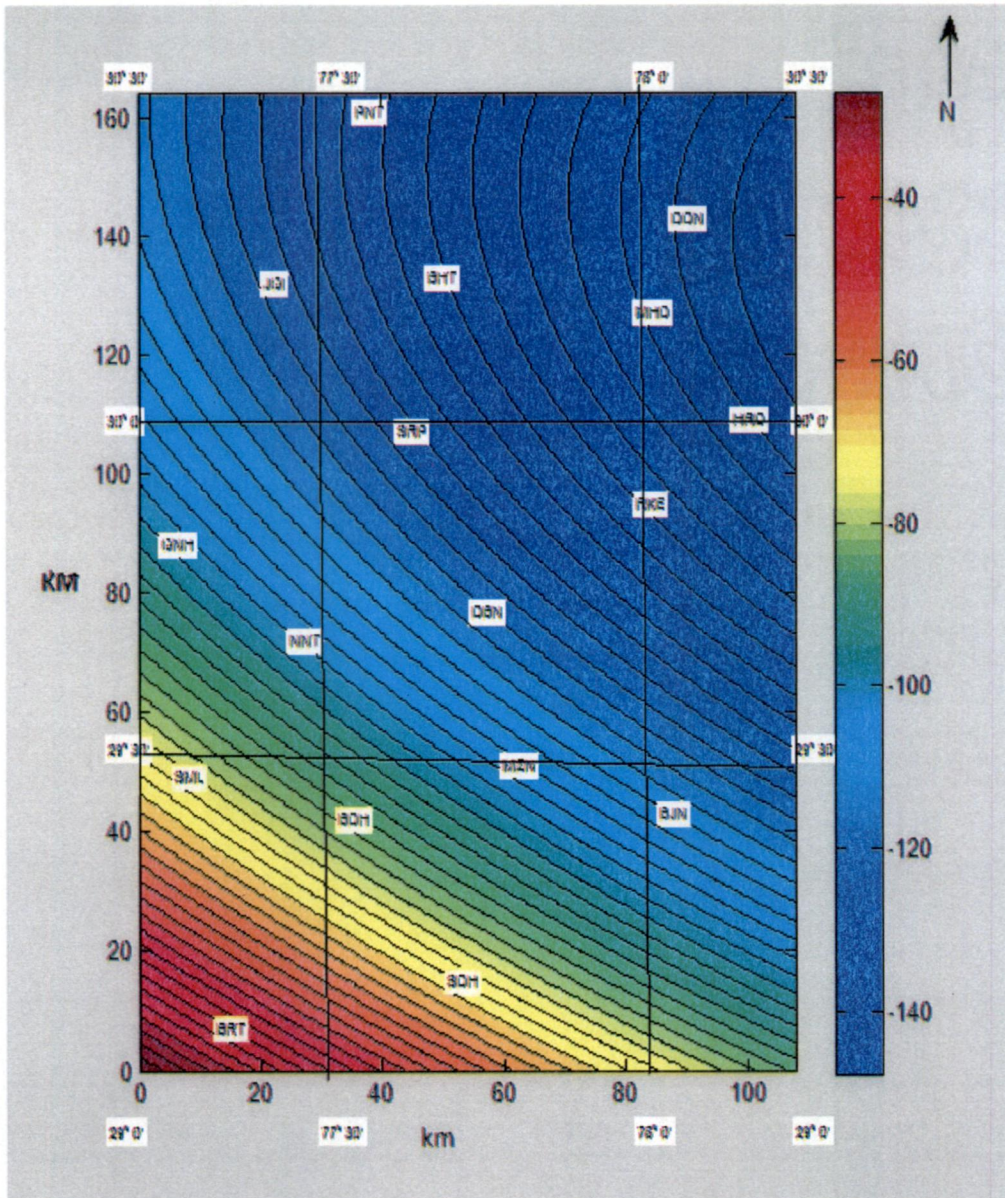
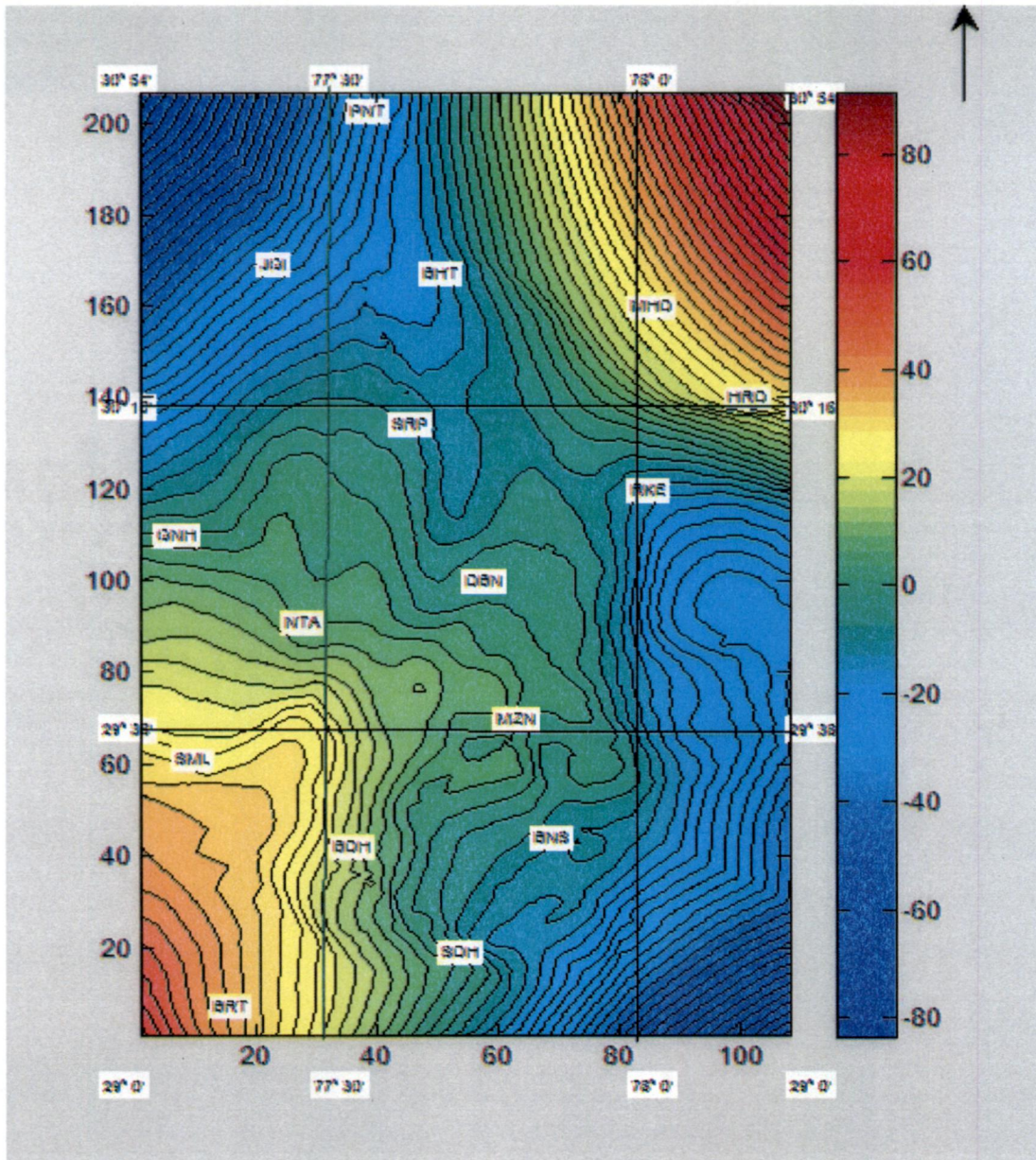Fig 5.4   Regional gravity map (derived using Second order Polynomial)

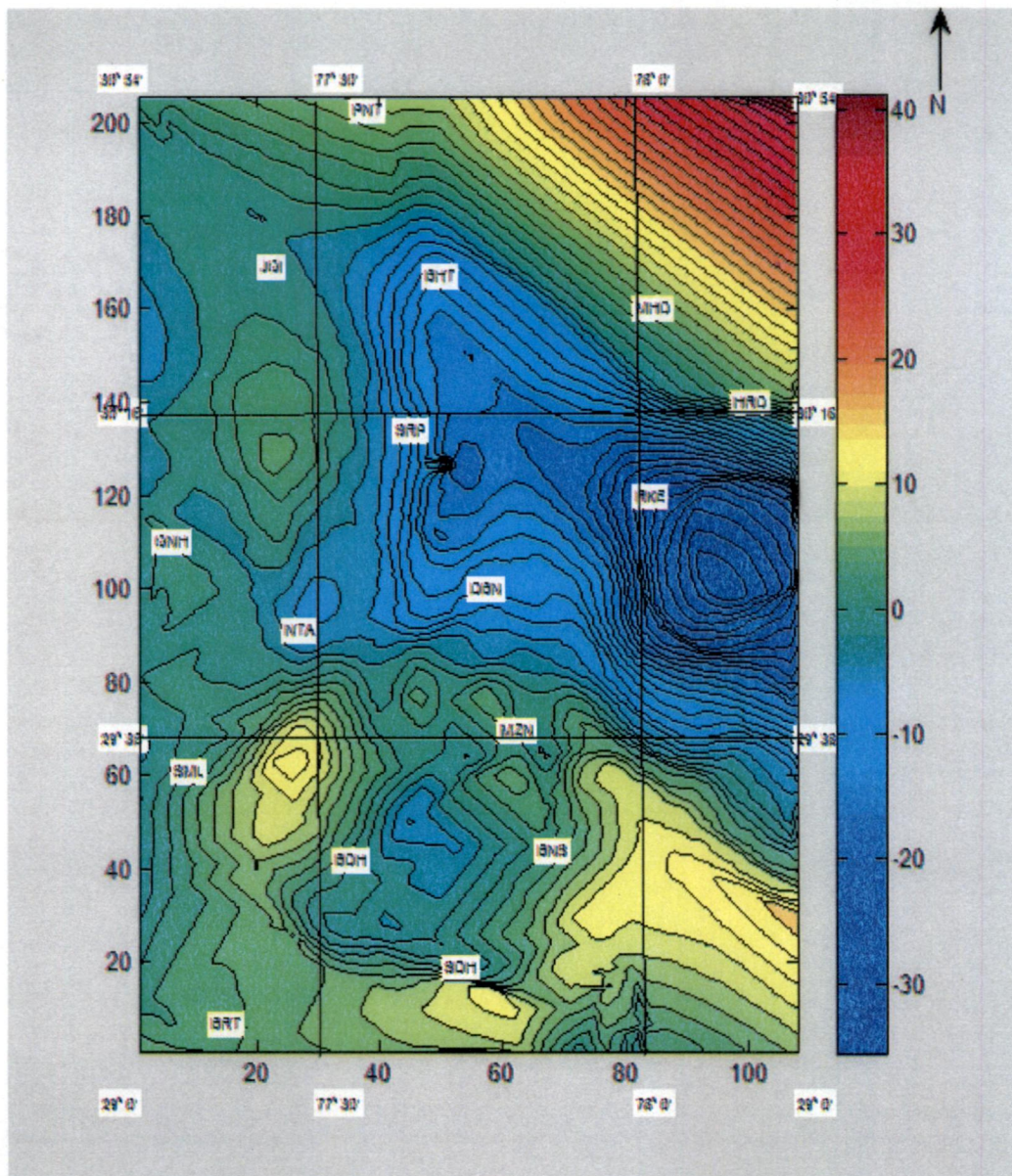Fig 5.5 Residual anomaly map using first order polynomial for regional

Fig 5.6 Residual anomaly map using Second order Polynomial for regional

5.3 Application of variable density 3D gravity inversion algorithm to IGP Data

To process the prepared residual anomaly data a rectangular mesh grid of dimension 108x164 sq. km is taken. So total 17712 grid nodes available for the processing of data. The grid spacing along x-axis and y-axis was taken 1 km for both. The value of constant of density function α was derived by fitting the known depth verses density data. It was carried out to be 0 .11gm/cc/km. Surface density contrast was taken to be -0.60gm/cc.

The adopted density model is shown in Fig 5.7. The value of damping factor was set initially 0.5, and the depth estimates improved iteratively according to algorithm. The modeled gravity data was again plotted in form of contour lines (shown in Fig 5.6) and the basement depth contour map has been also prepared for the interpretation part of the work

Computer program

A inversion code based on Matlab, has been given in the Appendix-1 Using this code one can obtain the depth contour map by providing necessary parameters.
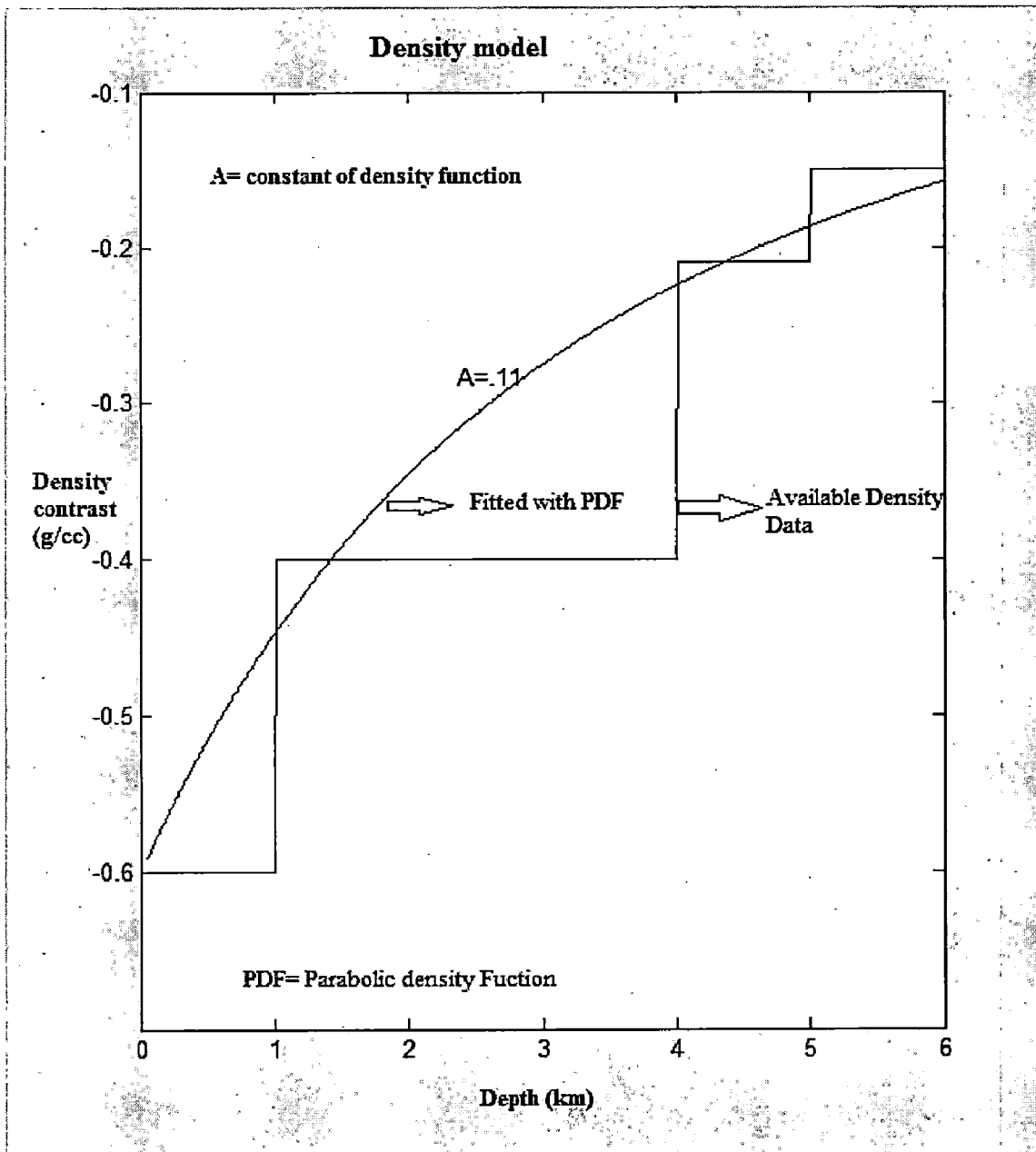
49

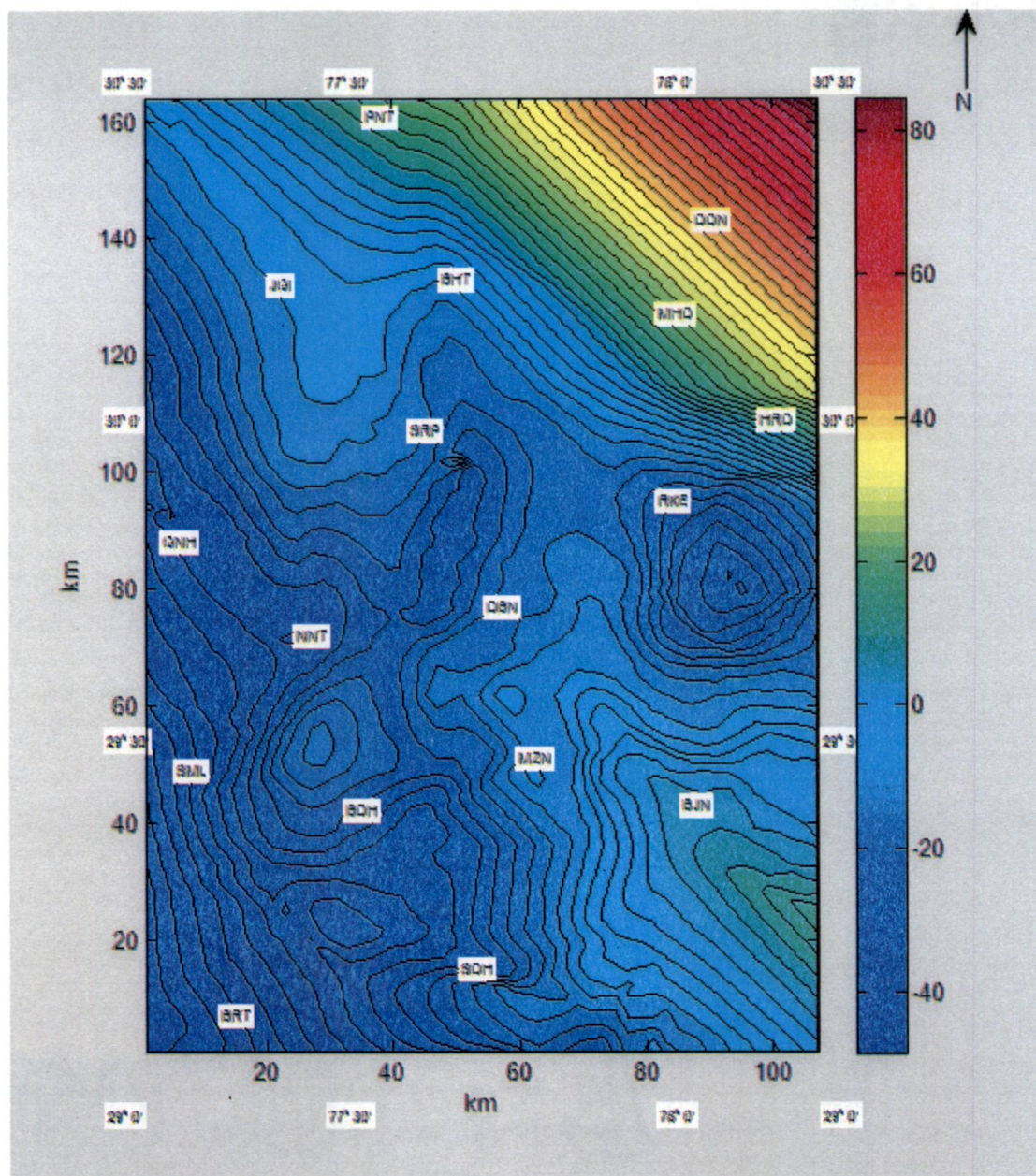Fig 5.7 Density variation depth model derived on the basis of Verma (1991)

Fig 5.8. Theoretical residual gravity anomaly data corresponding to closure criterian

CHAPTER -6

RESULTS AND DISCUSSIONS

6.1 Nature of residuals

The Bouguer anomaly map has been digitized and after digitization it has been reproduced using Matlab software and shown in Fig 5.2. The residual anomaly map has been produced using first order as well as second order polynomials and shown in Fig 5.5 and Fig 5.6 respectively. In Fig 5.6 one can see the positive centers in residual anomaly map. These positive centers in residual anomaly map seem to align themselves in an approximately NE-SW trend, suggesting a ridge-like feature. This kind of observation had led the previous authors to coin a term Delhi-Haridwar ridge. However a detailed interpretation could have revealed the complex nature of basement.

6.2 Basement Topography

To understand the nature of basement in the proposed area, the depth values at each grid node has been determined by the 3D inversion algorithm and a depth contour map (Fig 6.1) has been prepared using the Matlab Software. The depth contour map suggest that the basement is very complex

In the following some salient features of basement depth contour map are outlined:

(1) It can be seen clearly in the depth contour map that basement is having very complex nature, which is ridden with many faults, local highs and lows .This makes basement exhibiting the block like structures bounded by the various faults.
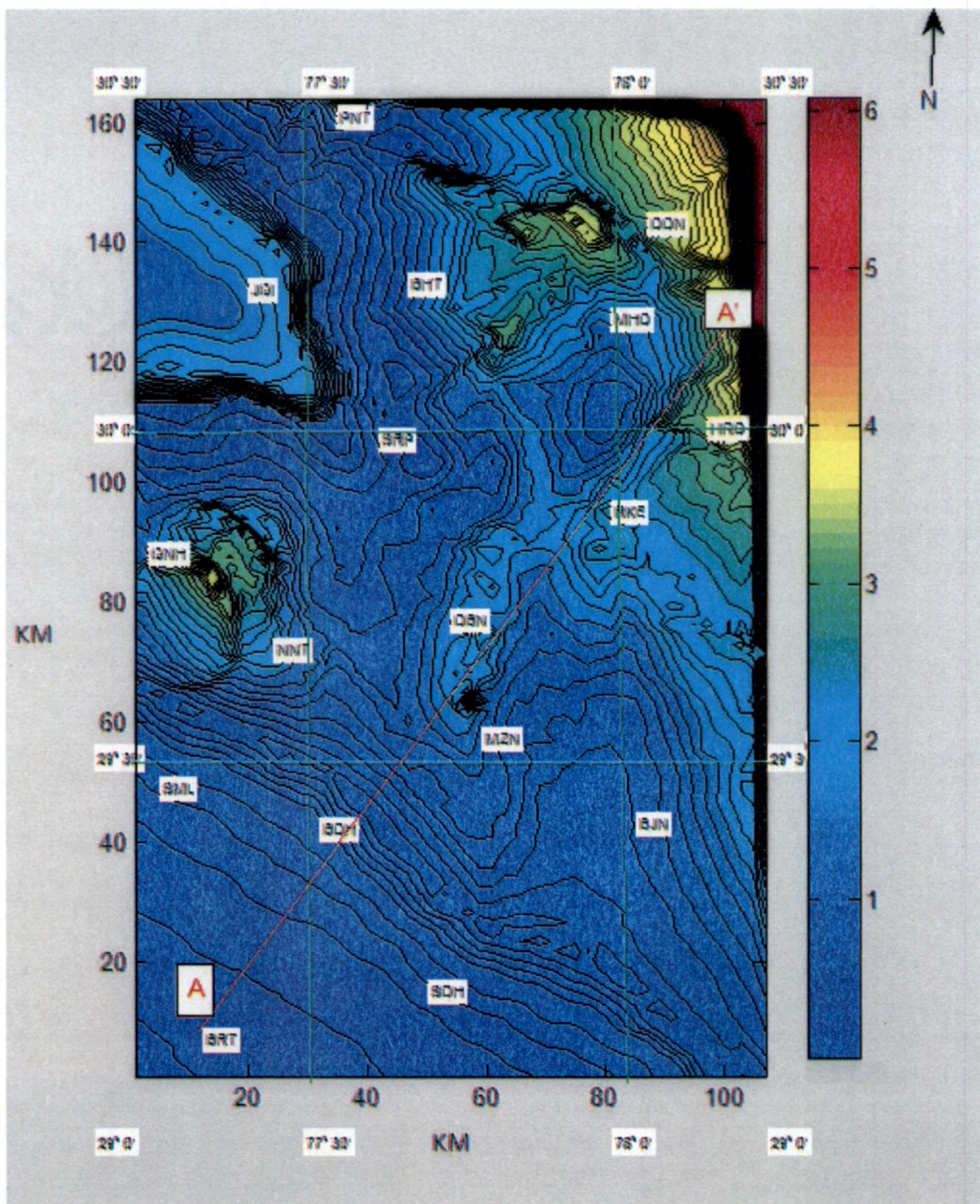
Fig 6.1 The basement depth contour map (Input data is residual gravity with second order polynomial for regional)

(2) Areas which are bounded by the faults have become the center of deposition of sediments. The depocentres are in the region around Gangoh(GNH) and Nanuta (NNT) , area around Deoband(DBN) and Muzaffarnagar (MFN)

(3) A large scale faults in the SW of Muzaffarnagar (MFN) and passing near to Budhana (BDH) follow the trend of HFT (Himalayan Frontal Thrust). This NW-SE trending fault at pre-tertiary basement level seems to cut orthogonally the nature across the supposed strike of Delhi- Haridwar Ridge.

(4) Transverse faults orthogonal to HFT are in the region around Deoband, Saharanpur and Behat.

(5) Presence of local highs and valleys make the basement look like Host and Graben like structures trend around Gangoh, Nanuta, Deoband and Muzaffarnagar area.

6.3 Limits and Nature of Delhi-Haridwar Ridge

To understand the nature of **Delhi-Haridwar** Ridge a profile AA′ has been taken. This profile passes through Baraut(BRT), Budhna(BDH), Muzaffarnagar(MZN,-Roorkee(RKE)-Mohand(MHD). Along this profile basement depth has been worked out and shown in Fig 6.2 with corresponding residual gravity anomaly value. A first look to residual anomaly map (Fig 5.4), the positive centers of residual anomaly seem to align themselves in an approximately NE-SW trend. This observation suggests a ridge like structures that was named in the literature as Delhi- Haridwar ridge. A close investigation has revealed the complex nature of the basement regarding this ridge.

(1) DHR seems to extend clearly upto Muzaffarnagar (MFN) in NE-SW direction (Sastry et al.,). Beyond that it can be seen along the profile that there is sudden change in basement depth. It can suggest that the tectonic forces came into play and it has influenced the nature of Pre-tertiary basement.

(2) It has been observed that SW of Deoband and Muzaffarnagar area, a major regional NW-SE trending fault at pre tertiary basement level is present which cut orthogonally across the supposed strike of DHR. This mean that DHR is best extended upto Deoband in NW-SE direction and the HFT related tectonics have been prevalent in Pre- tertiary basement much before its surface expression as the HFT

(3) Between Muzaffarnagar and Deoband the DHR turns gradually towards NW indicating a dextral oblique-slip component along the postulated fault. The similar interpretation was made in past by Sastry et.al (1999), which supports the results obtained here

(4) Interpreting the profile AA' suggests the general basement dipping trends in the NE-SW direction. This can also be observed by investigating the regional gravity map of first order polynomial. The negative anomaly is increasing in the NE-SW direction supporting the fact that basement has a general dipping trends along profile AA'

(5) Apart from the general trend of the DHR there are local upliftment and depressions in the ridge.

(6) In fig 6.2, along the profile AA' the obtained basement depth has been compared with the published one by Verma (1991). Red lines show the results obtained by the present work and green line shows basement depth given by Verma (1991). It is seen that basement topography along this profile is nearly similar in both cases.

(7) In Mohand area the estimated depth along this profile is around 4.4 km which is supported by the available depth (4.2 km) information from Mohand Deep well (Verma, 1991)

(8) Another geological control along profile BB' was provided by the seismic section near Muzaffarnagar area (Agrawal, 1977). The comparison of the results with the seismic information has been shown in the Fig 6.3
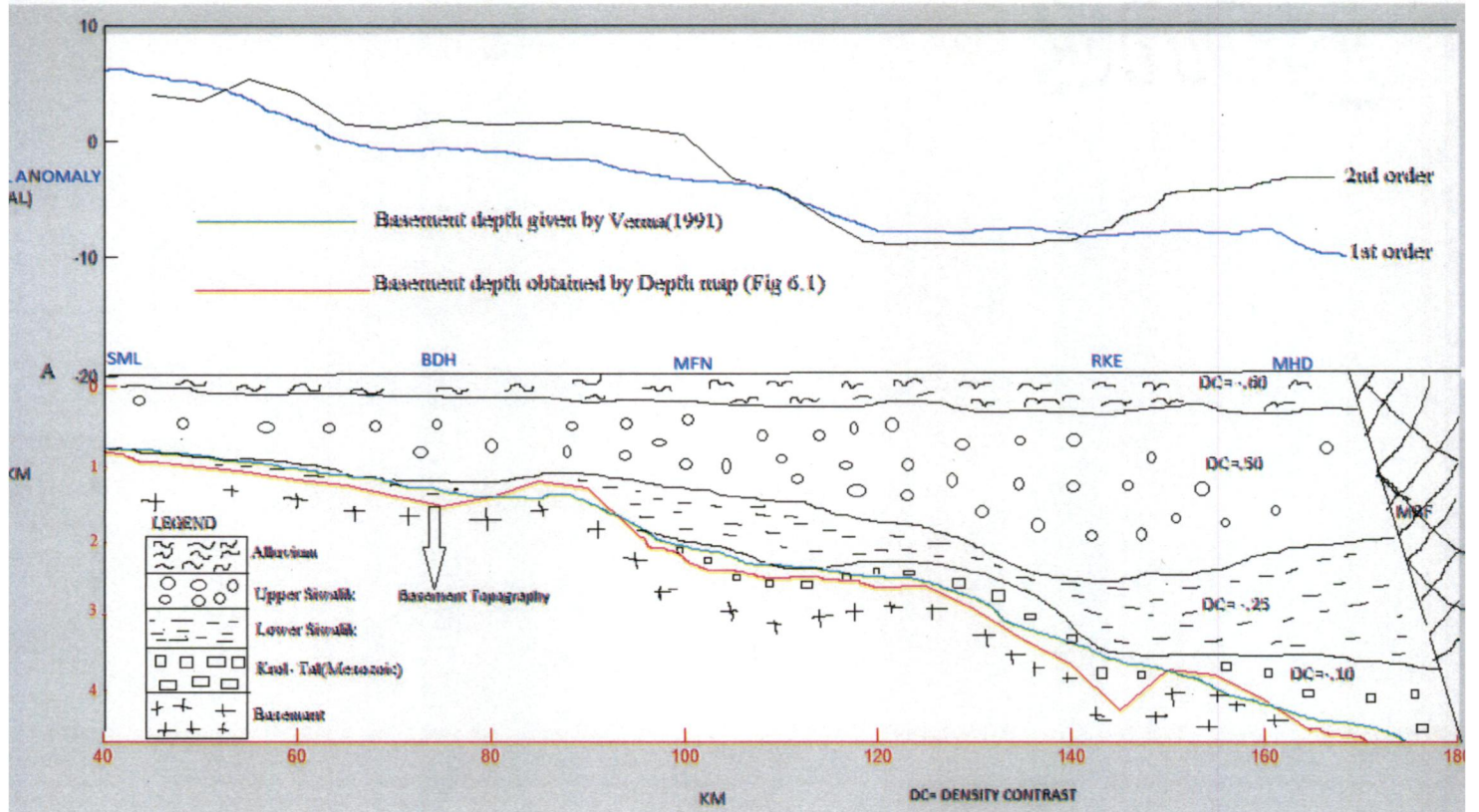
Fig 6.2 Basement Topography along Profile AA' (DHR)

(9) The available seismic section (Agrawal,1977) suggest that the basement depth varies from 0.8 km for Budhana to 1.32 km for Muzaffarnagar and 2.0 km for Purkaji, Further it assumes a P- wave velocity of 5.6 km/sec for the basement. The basement depth obtained by the gravity data, is 1.0 km for the Budhana, 1.84 km for the Muzaffarnagar, 2.32 km for Purkaji and it increases towards Roorkee- Haridwar area.

Fig 6.3 Comparison of basement depth along profile BB' with available seismic section (Agarwal, 1977)

a) Seismic section (Agarwal, 1977)

b) Gravity derived basement depths (BDH-Budhana, MZN-Muzaffarngar, PUR-Purkaji, RKE-Roorkee, HRD-Haridwar

6.4 Structural fabric derived from the Gravity data in the study region
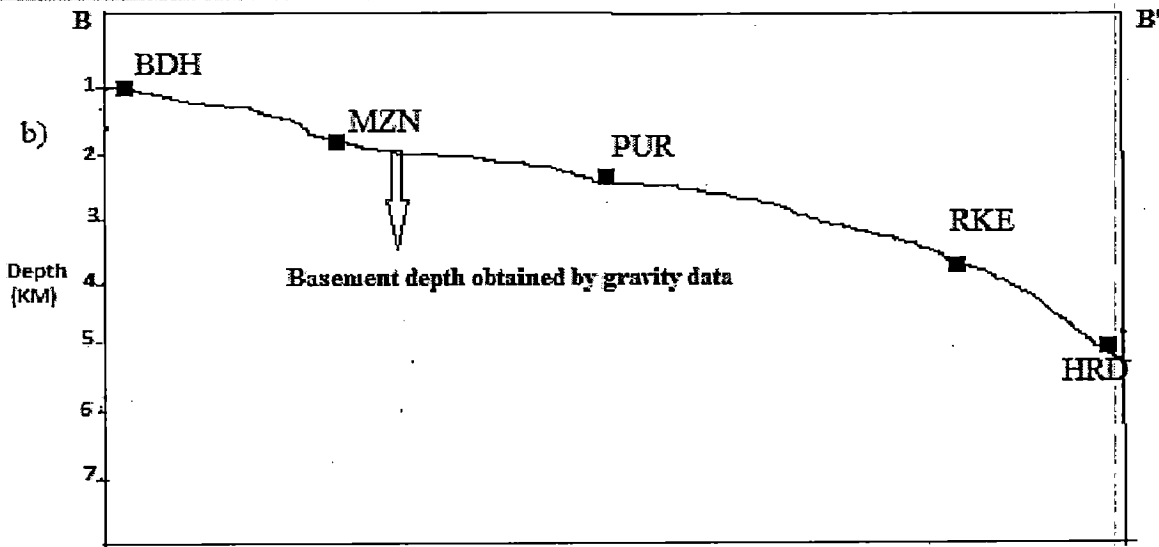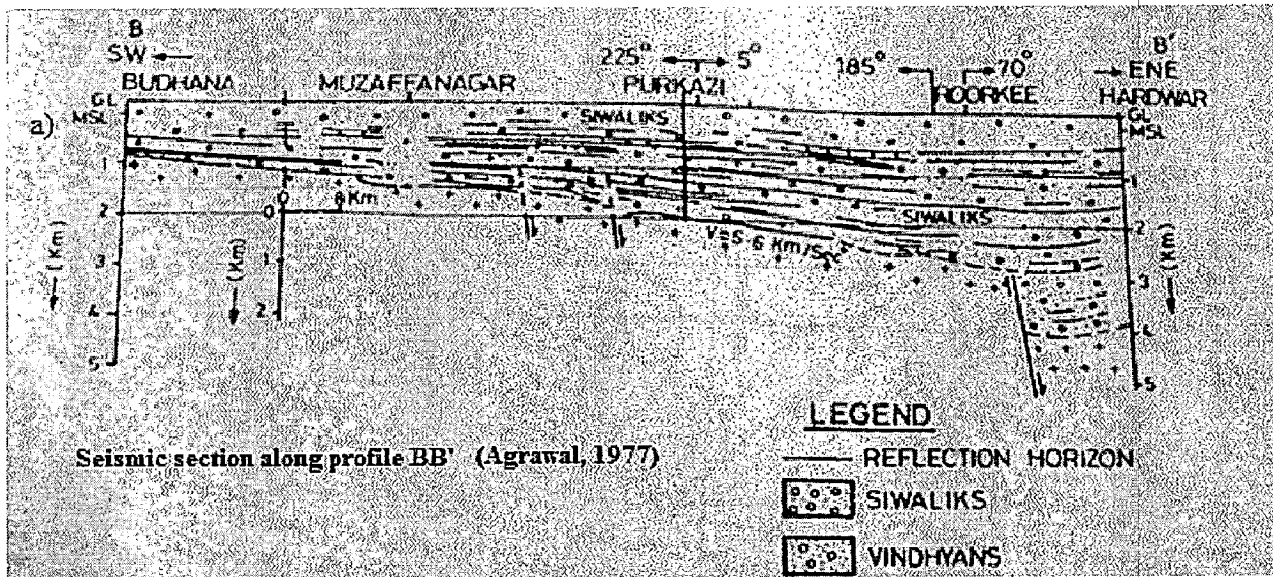
With the help of the obtained basement depth contour map locations of faults traces in the study region has been marked and shown in the Fig. 6.4. The major faults in this region are described below:

(1) There is a large scale regional fault (F1) having trend of NW-SE that cuts across the DHR, this fault is at shallow depth passing through Shamli (SML), Budhana (BDH), and Sardhana (SDH). The average depth of the fault is about 0.8 km.

(2) Faults F2 and F3 are around the Deoband giving Horst- like structure in the basement. Same kind of fault pattern is seen between Mohand (MHD) and Behat (BHT) area (F6&F7)

(4) Jagathri (JGI) region is also bounded by faults giving block like structure (F5). This area has become depocentre due to this fault.

(3) Fault (F4) surrounding the Nanauta (NNT) and Gangoh (GNH) area give the basement a block like structure. Due to this deep seated fault, this region has become center of large sedimentation. Average depth of this fault in this region is 4.3 km.

(4) There is another large scale fault passing through north of Bijnaur (BJN) passing in the west of Roorkee and extends in curviplanner manner upto Mohand area. The depth of the fault is varying, at Roorkee it is at 3.1 km, in east of Mohand it is about 4.7 km.

In Fig. 6.5 locations of faults zone has been delineated on a geological map. This area is a portion of our study region comprising Dehradun and Mohand region . The existence of regional faults prior to MBT in HFT region has been inferred. These faults zones were also inferred by Sastry et.al.(1999) from two sets of regional gravity and magnetic profiles on the geological map (Fig 1.5)
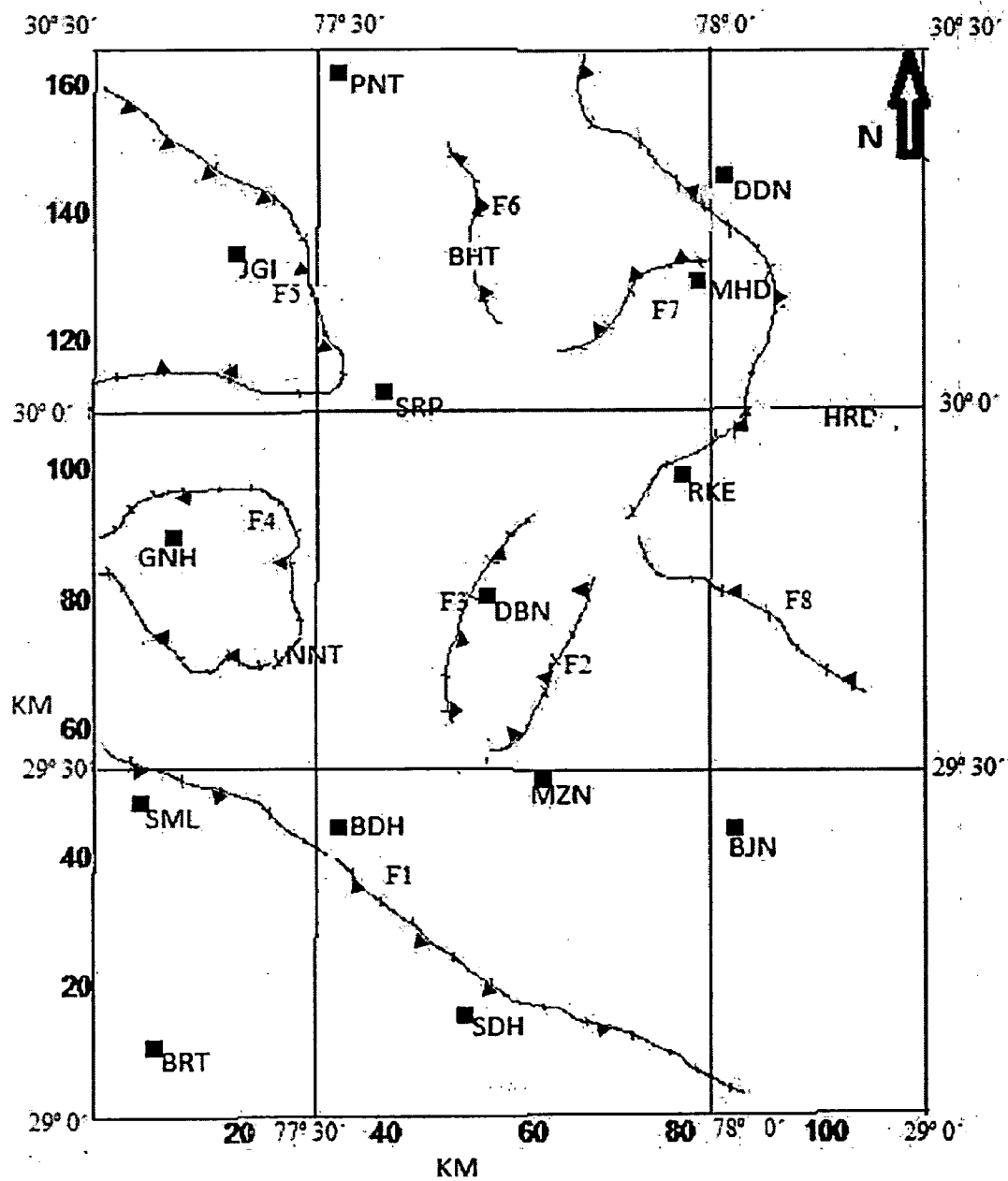
Fig 6.4 Derived Structural fabric from Fig 6.1 in the study region (BDH-BUDHANA, BRT-BARAUT, SDH-SARDHANA, SML-SHAMLI, NNT-NANAUTA, BJN-BIJNOR, MZN-MUZAFFAR NAGAR, GNH-GANGOH, DBN-DEOBAND, RKE-ROORKEE, HRD-HARIDWAR, SRP-SAHARANPUR, MHD-MOHAND, DDN-DEHRADUN, BHT- BAHAT, PNT-PAONTA), F1-F8 (Gravity interpreted basement fault)
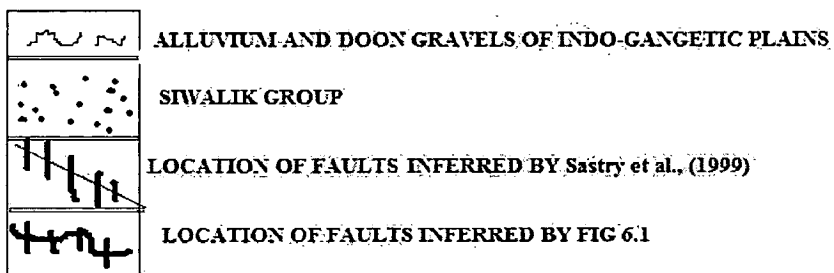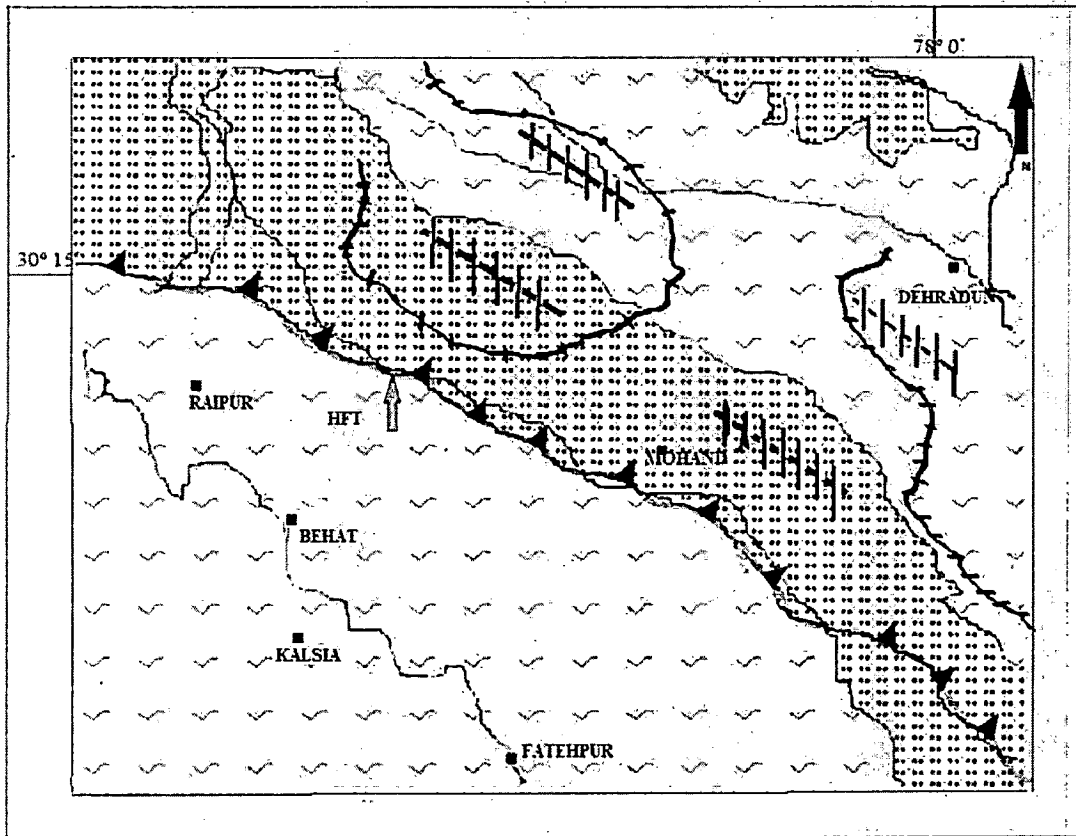
Fig 6.5 Inferred Locations of faults zones on geological map

Chapter- 7

Summary and Conclusion

Summary of the work

The whole thesis work can be summarized as follows:

(1) 3D Gravity inversion algorithm based on prism model that incorporates variable density contrast with depth of sedimentary basin (Parabolically)

(2) A published Bouguer anomaly data in Indo- Gangetic Plains was taken for the study of basement structure in the study region. Bouguer anomaly map has been digitized at 1 Km grid spacing in both East and North direction to make gravity value available on each grid nodes

(4)Two versions of residual anomaly maps have been separated from the regional anomaly using polynomial fitting method.

(5) Residual anomaly has been inverted by the algorithm and depths at each grid nodes have been obtained. Based on these depth values basement depth contour map has been prepared for the interpretation

Conclusions

(1) The interpretation of earlier obtained basement depth map reveals the general complex behavior of the basement. The basement exhibits block tectonics. It has very complex in nature and is composed of many faults, several local highs and lows.

(2) The basement depth values fairly agree with the available seismic section along the profile BB' (Fig)

(3) Existence of regional NW-SE trending fault in SW of Deoband and passing through near Budhana (Fig 6.4), seem to affect the Pre-tertiary basement. This suggest that the

HFT- related tectonics has affected the basement well before the surface expression of HFT

(4)The proposed Delhi-Haridwar ridge was studied and It was noticed that maximum northern limit of the DHR is upto Deoband region with clear expression upto Muzaffarnagar towards south. (Fig 6.1)

(5) Presence of regional thrust faults in HFT region are inferred from the Fig 6.1

(6) There sedimentary depocentres are inferred around Gangoh, Deoband, Jagathri and Behat area. (Fig 6.4)

References

1. Agarwal, R.K., 1977, Structure and tectonic of Indo-Gangetic plains, Aeg, Geophysical Case Histories, Volume -1, pp. 29-26.

2. Adriasyah, A., and A. G. McMechan, 2002, Analysis and interpretation of seismic data from thin reservoirs: Northwest Java basin, Indonesia: Geophysics,67, 14–26.

3. Bullard, S.G.,1915, Origin of Indo-Gangetic trough,commonly called Himalayan foredeep, Proc. Roy. Soc. Londan, V.91 A, pp. 220-238.

4. Chakravarthi, V., S. B. Singh, and G. A. Babu, 2001, INVER2DBASE —A program to compute basement depths of density interfaces above which the density contrast varies with depth: Computers & Geosciences, 27 , 1127–1133

5. Chakravarthi, V., H. M. Raghuram, and S. B. Singh, 2002, 3D forward gravity modeling of density interfaces above which the density contrast varies continuously with depth: Computers & Geosciences, 28, 53–57.

.6. Chakravarthi, V., and N. Sundararajan, 2004, Ridge regression algorithm for gravity inversion of fault structures with variable density: Geophysics, 69, 1394–1404.

7. Chakravarthi, V., and N. Sundararajan, 2006b, Gravity anomalies of 2.5-D multiple prismatic structures with variable density: A Marquardt inversion: Pure and Applied Geophysics,163, 229–242

8. Cordell, L., 1973, Gravity anomalies using an exponential density-depth function San Jacinto Graben, California: Geophysics,38, 684–690.

9. Dobrin, M.B., C.H. Savit, 1988, introduction to geophysical prospecting . Mc. Grass Hill Book Co.Ltd, page no-40

10. García- Abdeslem, J., 2005, The gravitational attraction of a right rectangular prism with density varying with depth following a cubic polynomial: Geophysics, 70 , no. 6, J39–J42

11. Götze, H. J., and B. Lahmeyer, 1988, Application of three-dimensional interactive modeling in gravity and magnetics: Geophysics, 53, 1096–1108

12. Holstein, H., and B. Ketteridge, 1996, Gravimetric analysis of uniform pol-hedra: Geophysics, 61, 357–364.

13. Karunakaran, C. and R. Rao, 1979, Status of hydrocarbon exploration in Himalayan region; contribution to stratigraphy and structure: Geol. Surv. India Misc, publ.no-41(5) pp-1-66.

14. Li, X., 2001, Vertical resolution: Gravity versus vertical gravity gradient: The Leading Edge, 20, 901–904.

15. Marquardt, D. W., 1963, An algorithm for least squares estimation of nonlinear parameters: SIAM Journal of Applied Mathematics, 11, 431–441.

16. Molnar, P.,1988, A review of geophysical constrants on the deep structure of thye tibbetian plateau, the Himalayas and the karakoram and their tectonic implications,Phil, Trans. R. Soc. Land. A 326, pp.33-38

17. Nagihara, S., and S. A. Hall, 2001, Three-dimensional gravity inversion using simulated annealing, constraints on the diapiric roots of allochthonous salt structures: Geophysics, 66, 1438–1449.

18. Prakash.B., Kumar.S., Rao,M.S.,Giri,S.C., Kumar and Gupta,S., 2001, Active tectonics of western Gangetic plain: In DST's spl. Vol.2 on seismicity, Ed. Verma, o.p.

19. Rao, D. B., 1990, Analysis of gravity anomalies of sedimentary basins by an asymmetrical trapezoidal model with quadratic density function: Geophysics,55, 226.

20 Rao, M.B.R.,1973, The subsurface geology of Indo-Gangetic Plains: Journal Geophysical society. Ind.V.14, No.35, pp. 217-242.

21. Sastri, V.V., Bhandari, L.L Raju ,A.T.P and A.K. ,Datta. 1971,Tectonic framework of subsurface stratigraphy of the ganga basin: Journal Geol. Society Of India Vol.12, No.3 pp.222-243

22. Sastry, R.G.S and P. R. Pujari and S. Lal, 1999, Basement structure below the indo-gangetic plains (IGP), Westren U.P., based on gravity and magnetic data: Gondwana research group ,Memoir 6, pp.321-327.

23. Singh, I.B., 1999, Tectonic control on sedimentation in Ganga Plain basin: constrants on siwalik sedimentation models: Gondwana Research Group memoir 6,pp. 247- 262.

24. Singh, B., and D. Guptasarma, 2001, New method for fast computation of gravity and magnetic anomalies from arbitrary polyhedral: Geophysics, 66, 521–526

25. Sengupta, S.N, 1977, Basement configuration of the Indo-Gangetic plains shown by aeromagnetic survey Aeg., Geophysical case histories, vol.1,pp.1-7

26 Talwani, M., and M. Ewing, 1960, Rapid computation of gravitational attraction of three-dimensional bodies of arbitrary shape: Geophysics, 25 ,203–225.

27. Wadia, D.N, 1957, Geology of India. Mc.Millan and Company Londan,pp.4, 388-389

Appendix-I

Computer program listing (Matlab) for gravity inversion and regional –residual separation

1) For 3D inversion Algorithm the code for Matlab Program is listed here

There are one main program and two supporting sub programs

```
(A) Main Program
clear all
clc
load Res;
load Gobs;
[M,N]=size(Gobs);SD=-0.6o;A=.11;K=M*N;
Z=-(SD*Res)./(41.89*SD+A*Gobs);
for s=1:P;
    [gcal]=GCAL(Z,SD,A);
    Jc=(Res(M,N)-gcal(M,N)).^2;
    J(s)=sum(sum(Jc));
    if s~=1
        if J(s)-J(s-1)>0
            lemda=2*lemda;
        else
            lemda=.5*lemda;
        end
    else
        lemda=0.5;
    end
    [GDIFF1]=Subp(Z,SD,Y-y,A);
    [GDIFF2]=Subp(Z,SD,y+y,A);
    GDIFF=.5*(GDIFF1+GDIFF2);
    ef=1;
    for u=1:N
        for v=1:M
            w=1;
            sh=GDIFF(:,:,u,v);
            B=(GOBS-gcal)*sh;
            BS(ef)=sum(sum(B));
            for j=1:N
                for k=1:M
                    if ((j==u)&&(k==v))
```

```
                    del=1;
               else
                    del=0;
               end

A1=GDIFF(:,:,u,v)*GDIFF(:,:,j,k)*(1+lemda*del);
               AS(ef,w)=sum(sum(A1));
               w=w+1;
          end
     end
     ef=ef+1;
   end
  end
  dz=AS.^(-1)*BS';
  dzt=reshape(dz,M,N);
  dzm=(dzt)';
  Z = Z+dzm;
end
```

(B) Sub program Gcal calculate theoretical gravity of basin

```
function [gcal]=GCAL(Z,SD,A)
[M,N]=size(Z);
for n=1:N;
    for m=1:M;
        SG=0;
        for k=1:N;
            for l=1:M;
                Z1=Z(l,k);
                dx=1;
                dy=1;
                X=abs(n-k)*dx;
                Y=abs(m-l)*dy;
                T=dx/2;
                HY=dy/2;
                Y1=HY-Y;
                Y2=HY+Y;
                [GPRM1]=GPRM(X,T,Y1,Z1,SD,A);
                [GPRM2]=GPRM(X,T,Y2,Z1,SD,A);
                GPRM=.5*(GPRM1+GPRM2);
```

```
                SG=SG+GPRM;
            end
        end
        gcal(m,n)=SG;
    end
end
```

(C) Subprogram GPRM that calculate the gravity response of a single prism

```
function [GPRM]=GPRM(X,T,Y,Z,SD,A)
if Z==0
    Z2=.0001;
else
    Z2=Z;
end
DC=13.33*(-0.67).^3;
Z1=0.0001;
AL5=SD-A*Z1;
AL6=SD-A*Z2;
Q1=X+T;
Q2=X-T;
R1=(Q1.^2+Y.^2+Z1.^2).^(.5);
R2=(Q2.^2+Y.^2+Z1.^2).^(.5);
R3=(Q2.^2+Y.^2+Z2.^2).^(.5);
R4=(Q1.^2+Y.^2+Z2.^2).^(.5);
T1=1/A;
T2=(atan((Y*Q1)/(Z2*R4)))/AL6-(atan((Y*Q1)/(Z1*R1)))/AL5;
TTR1=T1*T2;
TT2=(atan((Y*Q2)/(Z2*R3)))/AL6-(atan((Y*Q2)/(Z1*R2)))/AL5;
TTR2=T1*TT2;
TER1=TTR1-TTR2;
T3=Y*Q1;
AL8=sqrt((Q1.^2+Y.^2)*A.^2+SD.^2);
T41=A*(2*SD.^2+A.^2*(Q1.^2+Y.^2));
T42=AL8*(Y.^2*A.^2+SD.^2)*(Q1.^2*A.^2+SD.^2);
T4=T41/T42;
T51=AL5*(A*R4*AL8+AL8.^2-SD*AL6);
T52=AL6*(A*R1*AL8+AL8.^2-SD*AL5);
T5=log(T51/T52);
TER2=T3*T4*T5;
T61=SD/(A*(SD.^2+Y.^2*A.^2));
T62=atan((Y*R4)/(Z2*Q1))-atan((Y*R1)/(Z1*Q1));
TER3=T61*T62;
```

```
T71=SD/(A*(SD.^2+Q1.^2*A.^2));
T72=atan((Q1*R4)/(Z2*Y))-atan((Q1*R1)/(Z1*Y));
TER4=T71*T72;
T81=Y/(2*(SD.^2+Y.^2*A.^2));
T82=log(((Q1-R4)*(Q1+R1))/((Q1+R4)*(Q1-R1)));
TER5=T81*T82;
T91=Q1/(2*(SD.^2+Q1.^2*A.^2));
T92=log(((Y-R4)*(Y+R1))/((Y+R4)*(Y-R1)));
TER6=T91*T92;
T101=SD/(A*(SD.^2+Y.^2*A.^2));
T102=atan((Y*R3)/(Z2*Q2))-atan((Y*R2)/(Z1*Q2));
TER7=T101*T102;
T111=SD/(A*(SD.^2+Q2.^2*A.^2));
T112=atan((Q2*R3)/(Z2*Y))-atan((Q2*R2)/(Z1*Y));
TER8=T111*T112;
T122=log(((Q2-R3)*(Q2+R2))/((Q2+R3)*(Q2-R2)));
TER9=T81*T122;
T131=Q2/(2*(SD.^2+Q2.^2*A.^2));
T132=log(((Y-R3)*(Y+R2))/((Y+R3)*(Y-R2)));
TER10=T131*T132;
AL4=sqrt((Q2.^2+Y.^2)*A.^2+SD.^2);
T141=Y*Q2;
T142=A*(2*SD.^2+A.^2*(Q2.^2+Y.^2));
T143=AL4*(Y.^2*A.^2+SD.^2)*(Q2.^2*A.^2+SD.^2);
T144=AL5*(A*R3*AL4+AL4.^2-SD*AL6);
T145=AL6*(A*R2*AL4+AL4.^2-SD*AL5);
TER11=((T141*T142)/(T143))*log(T144/T145);
G=TER1+TER2-TER3-TER4+TER5+TER6+TER7+TER8-TER9-TER10-TER11;
GPRM=DC*G;
```

(2)
Program for Regional residual -speration

2a) For first order polynomial fitting for regional

```
load g
m=108;
n=206;
[x,y] = meshgrid(1:1:108,1:1:206);
sg=sum(sum(g));
sx=sum(sum(x));
```

```
sy=sum(sum(y));
x2=x.*x;
y2=y.*y;
xy=x.*y;
gx=g.*x;
gy=g.*y;
sx2=sum(sum(x2));
sy2=sum(sum(y2));
sxy=sum(sum(xy));
sgx=sum(sum(gx));
sgy=sum(sum(gy));
c1=[sx,sy,m*n;sx2,sxy,sx;sxy,sy2,sy];
c2=[sg;sgx;sgy];
c3=c1^(-1)*c2;
A=c3(1,1);
B=c3(2,1);
C=c3(3,1);
R=A*x+B*y+C;
Res=g-R;
```

2b) Program for Second order polynomial fitting for regional

```
% Second Order polynomial(A*x2+B*y2+C*xy+D*x+E*y+F=R)
load gdata
[m,n]=size(gdata);
mn=m*n;
[x,y] = meshgrid(1:1:108,1:1:206);
x2=x.*x;      y2=y.*y;      xy=x.*y;
x3=x2.*x;     x2y=x2.*y;    xy2=x.*y2;
y3=y2.*y;     x4=x3.*x;     x2y2=x2.*y2;
x3y=x3.*y;    xy3=x.*y3;    y4=y3.*y;
g=gdata;      gx=g.*x;      gy=g.*y;
gx2=g.*x2;    gy2=g.*y2;    gxy=g.*xy;
sg=sum(sum(g)); sgx=sum(sum(gx)); sgy=sum(sum(gy));
sgx2=sum(sum(gx2)); sgxy=sum(sum(gxy)); sgy2=sum(sum(gy2));
sx=sum(sum(x));  sy=sum(sum(y));  sxy=sum(sum(xy));
sx2=sum(sum(x2));   sy2=sum(sum(y2));   sx3=sum(sum(x3));
sx2y=sum(sum(x2y)); sy3=sum(sum(y3));   sx4=sum(sum(x4));
```

```
sx2y2=sum(sum(x2y2));    sx3y=sum(sum(x3y));
sxy3=sum(sum(xy3));
sy4=sum(sum(y4));sxy2=sum(sum(xy2));
G=[sx2,     sy2,     sxy,     sx,     sy,      mn;
   sx3,     sxy2,    sx2y,    sx2,    sxy,     sx;
   sx2y,    sy3,     sxy2,    sxy,    sy2,     sy;
   sx4,     sx2y2,   sx3y,    sx3,    sx2y,    sx2;
   sx2y2,   sy4,     sxy3,    sxy2,   sy3,     sy2;
   sx3y,    sxy3,    sx2y2,   sx2y,   sxy2,    sxy];
SGD=[sg; sgx; sgy; sgx2; sgy2; sgxy];
M=G^(-1)*SGD;
A=M(1); B=M(2); C=M(3); D=M(4); E=M(5); F=M(6);
R=A*x2+B*y2+C*xy+D*x+E*y+F;
RESS=R-g;
```